HHS Public Access

Author manuscript

J Comp Neurol. Author manuscript; available in PMC 2022 October 01.

Published in final edited form as:

J Comp Neurol. 2021 October ; 529(14): 3389–3409. doi:10.1002/cne.25198.

Macaque Monkey Trigeminal Blink Reflex Circuits Targeting Levator Palpebrae Superioris Motoneurons

Susan Warren, **Paul J. May**

Department of Neurobiology and Anatomical Sciences, University of Mississippi Medical Center, Jackson, MS, 39216

Abstract

For normal viewing, the eyes are held open by the tonic actions of the levator palpebrae superioris (levator) muscle raising the upper eyelid. This activity is interrupted during blinks, when the eyelid sweeps down to spread the tear film or protect the cornea. We examined the circuit connecting the principal trigeminal nucleus to the levator motoneurons by use of both anterograde and retrograde tracers in macaque monkeys. Injections of anterograde tracer were made into the principal trigeminal nucleus using either a stereotaxic approach or localization following physiological characterization of trigeminal second order neurons. Anterogradely labeled axonal arbors were located both within the caudal central subdivision, which contains levator motoneurons, and in the adjacent supraoculomotor area. Labeled boutons made synaptic contacts on retrogradely labeled levator motoneurons indicating a monosynaptic connection. As the eye is also retracted through the actions of the rectus muscles during a blink, we examined whether these trigeminal injections labeled boutons contacting rectus motoneurons within the oculomotor nucleus. These were not found when the injection sites were confined to the principal trigeminal nucleus region. To identify the source of the projection to the levator motoneurons, we injected retrograde tracer into the oculomotor complex. Retrogradely labeled cells were confined to a narrow, dorsoventrally oriented cell population that lined the rostral edge of the principal trigeminal nucleus. Presumably these cells inhibit levator motoneurons, while other parts of the trigeminal sensory complex are activating orbicularis oculi motoneurons, when a blink is initiated by sensory stimuli contacting the face.

Tonic activity in the levator palpebrae superioris muscle, which holds the upper eyelid open, is interrupted during blinks. Here we demonstrate a monosynpatic pathway from cells distributed along the rostral edge of the principal trigeminal nucleus that targets, and presumably inhibits, levator motoneurons for blinks triggered from the face.

Graphical Abstract

Send correspondence to: Paul J. May, PhD, Department of Neurobiology & Anatomical Sciences, University of Mississippi Medical Center, 2500 North State Street, Jackson, MS 39216, pmay@umc.edu, Phone: 601-984-1662, Fax: 601-984-1655

Contributions: The experiments were designed by PJM & SW, recordings were made by SW, data was analyzed by SW & PJM, figures were prepared by PJM & SW, the manuscript was drafted by PJM and edited by PJM & SW.

Conflict of Interest: Neither author has any conflicts of interest, financial or otherwise, with respect to the work described in this manuscript.

Data Sharing: The data supporting this study are available for loan upon reasonable request to the authors.

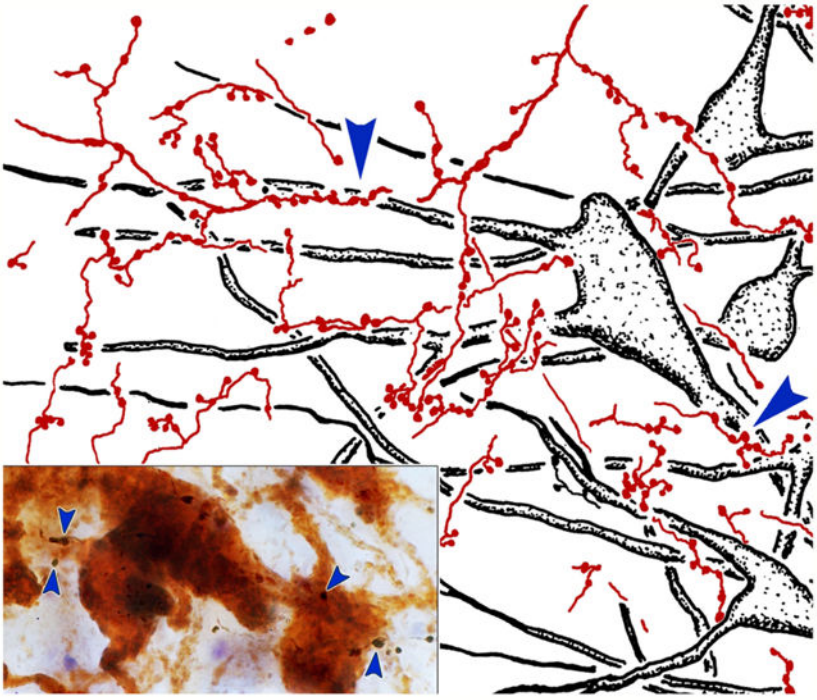

Keywords

oculomotor; trigeminal; primate; eyelid; somatosensory; apraxia of lid opening

INTRODUCTION

Each morning, upon awakening, we open our eyes to greet the world. And each evening, we close them to disconnect from visual sensory input in preparation for sleep. In between, the lids are actively held open, even though we are little aware of muscular exertion producing this effect. The volitional and reflex actions of the eyelid are governed by an antagonist pair of striated muscles: the orbicularis oculi muscle and the levator palpebrae superioris (hence forth levator) muscle. It is the levator muscle that holds the upper eyelid open for viewing during the day. Indeed, the fiber types within the levator are appropriate for this sustained action (Porter et al., 1989). It is assisted in keeping the eyes open by the smooth muscle slips of the superior and inferior tarsal muscles. Changes in levator muscle activity also raise and lower the upper eyelid during vertical gaze changes, so that during vertical eye movements it always sits just above the pupillary margin, at the ready for a protective blink, (monkey: Becker and Fuchs, 1988; human: Guitton et al., 1991). During a blink, levator muscle action is suppressed during the closing phase, while the orbicularis oculi muscle closes the eyelids, and then reinstated to produce the opening phase of the blink (Becker and Fuchs, 1988; Porter et al., 1993; Aramideh et al., 1995). Similarly, levator motoneuron activity is sharply suppressed during the closing phase of a blink (Fuchs et al., 1992). Thus, in contradistinction to the blink-related, phasic activity of the orbicularis motoneurons, levator motoneurons display tonic activity that is modulated with respect to gaze position and blinks (Fuchs et al., 1992). The importance of the tonic signal on levator motoneurons is indicated

by the effects of the loss of levator muscle action in “apraxia of lid opening” (Schmidtke & Büttner-Ennever, 1992; Aramideh et al., 1995; Boghen, 1997; Defazio et al., 1998); the eyelids close involuntarily, rendering the patient temporarily sightless.

The motoneurons controlling the actions of the levator muscle are located in the caudal central subdivision (CC) of the oculomotor nucleus (III). Among the species that have been investigated, this subdivision is an unpaired nucleus found on the midline dorsal to the caudal pole of III in frontal eyed animals (cat: Akagi, 1978; Chen and May, 2002; galago: Sun and May, 1993; monkey; Porter et al., 1989; Jamilah et al., 1992; VanderWerf et al., 1997), but is arranged as a pair of motoneuron pools located at the lateral edge of III in lateral eyed animals (rat: Glicksman, 1980; Labandeira Garcia et al., 1983; rabbit: Akagi, 1978; Murphy et al., 1986; van Ham and Yeo, 1996; guinea pig: Gomez Segade and Garcia, 1983). The organization of the monkey CC is noteworthy for the nearly balanced bilateral distribution of the motoneurons (Porter et al., 1989), as blinks and vertical gaze-related eyelid movements are generally paired in frontal eyed species (Becker and Fuchs, 1988; Porter et al., 1993). Indeed, it appears that some levator motoneurons actually project bilaterally in frontal eyed species (cat: May et al., 2012; monkey: Sekiya et al., 1992; VanderWerf et al., 1997). Levator motoneurons fire in a manner quite similar to superior rectus motoneurons during vertical gaze movements (monkey: Fuchs et al., 1992), when the eye and lid position move in parallel (monkey: Becker and Fuchs, 1988; Guitton et al., 1991; human: Bour et al., 2000). There is good evidence that these two groups of motoneurons receive similar inputs from vertical gaze centers. An area adjacent to the rostral interstitial nucleus of the medial longitudinal fasciculus, termed the M-group in monkeys, projects to the levator motoneurons in CC (cat: Chen and May, 2002; monkey: Horn et al., 2000), and these motoneurons also get input from the interstitial nucleus of Cajal (cat: Chen and May, 2007). Both these upgaze motoneuron pools are also histochemically characterized by the presence of calretinin in many of the terminals contacting them from the vertical gaze centers (monkey: Ahlfeld et al., 2011; Zeeh et al., 2013; human: Che Ngwa et al., 2014; Adamczyk et al., 2015).

As noted by Fuchs and colleagues (1992) the activity in levator motoneurons differs substantially from that of superior rectus motoneurons during a blink closing phase. During this movement, action potentials in the levator motoneurons are significantly suppressed, but the activity in superior rectus motoneurons is not inhibited. Levator motoneuron firing returns during the opening phase of the blink. Indeed, as noted by Gruart and Delgado-Garcia (1994) in their examination of blink-related activity in cerebellar cortex neurons, it is important to consider the actions of the levator muscle and the circuitry controlling it in order to have a full understanding of the trigeminal blink reflex (see also Evinger et al., 1991; Sibony et al., 1991). Based on a cat study, it has been suggested that inhibition of levator motoneurons during the trigeminal blink reflex is produced by a set of neurons associated with the exiting facial and trigeminal nerves and lying immediately rostral and ventral to the principal trigeminal nucleus (pV) and ventral to pars oralis of the spinal trigeminal nucleus (sVo) (May et al., 2012). This trigemino-oculomotor projection has also been described in the rabbit (Guerra-Seijas et al., 1993; van Ham and Yeo, 1996). In the present study, we used dual tracer techniques to examine whether the rostral region of the

trigeminal sensory nucleus provides input to levator motoneurons in macaque monkeys. We further examined the precise source of this projection by using retrograde tracers.

Alternatively, it has been suggested that this trigemino-oculomotor projection is an excitatory one that targets the rectus motoneurons to produce retraction of the eye ball during a blink, and some have suggested that it results in Bell's phenomenon (cat: Ogasawara, 1985; rabbit: Guerra-Seijas et al., 1993). In the present macaque experiments, we discriminated between these possibilities by also examining whether there are projections from the rostral region of trigeminal sensory nucleus to superior or medial rectus motoneurons in III.

METHODS

These experiments were performed on 9 monkeys, including both *Macaca mulatta* (n=3) and *Macaca fascicularis* (n=6) subjects. Both male (n=4) and female (n=5) animals were used. We did not observe any pattern of differences in the connectional results that could be attributed to species or sex. All procedures were designed in agreement with the recommendations of the Guide for Care and Use of Laboratory Animals, and the surgical protocols were approved by the Institutional Animal Care and Use Committee of the University of Mississippi Medical Center. Prior to surgical procedures, animals were first sedated with ketamine HCl (10 mg/kg, IM). They were then intubated and a surgical level of anesthesia was induced with an oxygen mixture of 1-3% isoflurane. An IV line was employed to ensure proper hydration. Excess production of mucus was inhibited with atropine HCl sulfate (0.05 mg/kg, IM). In addition, dexamethasone (2.5 mg/kg, SC) was employed to suppress brain edema. Temperature and respiration were monitored and kept within normal ranges. The animals' heads were stabilized within a stereotaxic frame during the surgery. Following surgery, the incision edges were infused with Sensorcaine and the animals received an analgesic, buprenorphine HCL (0.01 mg/kg).

Stereotaxic Injections of pV

Stereotaxic injections of pV (n=5) (Paxinos et al., 2000) were made after aspirating the overlying cortex to allow visualization of the pontomesencephalic junction. Specifically, following a craniotomy, the medial part of the left occipital lobe was aspirated to reveal the rostral edge of tentorium cerebelli and adjoining tectum. The tentorium was incised, and the cerebellar cortex was gently separated from the caudolateral edge of the inferior colliculus to reveal the middle cerebellar peduncle and overlying trochlear nerve. The nerve and the junction between the peduncle and tegmentum were used as landmarks for the access point of a 5 μl Hamilton syringe that was angled 1–2° tip medial in the frontal plane. The needle was advanced 4.0-4.5 mm into the brainstem to reach pV. At this point, 0.1-0.5 μl of 10.0% biotinylated dextran amine (BDA) was injected, sometimes spreading the injection sites over a 1.0 mm range, while withdrawing the needle. In an additional control animal (n=1), the injection was placed more laterally, so that it just included the middle cerebellar peduncle and the exiting trigeminal nerve. The aspiration defect was then filled with hydrated Gelfoam and the scalp was reapproximated and sutured with vicryl. These animals survived for 21 days after the BDA injection to allow anterograde tracer transport.

Muscle Injections

In 4 of the 5 pV stereotaxic injection cases, extraocular muscles were injected 19 days after the BDA injection to retrogradely label their motoneurons. Animals were prepared for surgery as described above. Then, the skin above the left brow was incised and retracted to allow visualization of the orbicularis oculi muscle. This muscle was incised along the supraorbital ridge, providing access to the orbital contents. Blunt dissection was used to isolate the levator muscle (n=4), the superior rectus muscle (n=3) and/or the medial rectus muscle (n=2). These were temporarily lassoed with a piece of suture to allow them to be stabilized during the injection. A 10 μl Hamilton syringe was used to inject the tracer, a combination of 1.0% wheat germ agglutinin conjugated horseradish peroxidase (WGA-HRP) and 5.0% horseradish peroxidase. We injected a total of 7 μl of this solution into the levator and 10 μl into each of the rectus muscles, moving the needle from place to place in order to spread the tracer through the muscle belly. The palpebral portion of the orbicularis oculi muscle was then reattached to the orbital portion with suture, and the skin of the eyelid was reapproximated and stabilized with suture. In some cases, other muscles were injected for other experiments that did not interfere with interpretation of the results presented here. The animals survived another 2 days to allow retrograde transport of the tracer.

Physiological Recording and Injection of pV

We instrumented one animal for awake behaving recording in order to localize pV before injecting 10% BDA. Using Bregma as a guide, a 20 mm diameter craniotomy straddling the midline was created for placement of a stainless steel recoding chamber to bilaterally access pV. The front of the chamber (24 mm ID, 36 mm OD) was aligned 14 mm anterior to frontal plane zero, with the back end angled ~ 18 degrees below horizontal. Stainless steel screws, were placed in the bone to support and anchor the chamber in a foundation of dental acrylic. A headholder assembly consisting of two inverted stainless steel screws was positioned in the dental acrylic foundation and located at the back of the skull. A removable silicon insert, which could be threaded into the chamber, offered protection to the underlying dura, and could be easily removed to allow recording. An acrylic cap protected the insert. In order to reach pV, a guide tube of stainless steel hypodermic tubing (22 gauge, ~ 50-60 mm in length; 0.016 inch IO, 0.028 inch OD) was used. The length was determined by calculating the distance from the cortical surface to pV (~30 mm) and adding the length of the microdrive head attachment (~14 mm) and chamber to skull distance (~16 mm). For a recording session, a sterilized guide tube was installed in the hydraulic microdrive (David Kopf Instruments) and introduced transdurally. The tube, contained a back-loaded, varnish-coated metal microelectrode (50mΩ, Fred Haer Inc). The microelectrode containing guide tube was positioned at a predetermined location using a polar coordinate system. It was lowered from the guide tube in ~500 micron increments to isolate spontaneous and drivable cell activity. Once activity restricted to the face was identified, the microelectrode was advanced in smaller increments. The neural signal from the microelectrode passed to head stage pre-amplifier and then an amplifier (BAK A/C differential amplifier). The amplified signal was passed through a window discriminator (BAK) and fed to an audio monitor (Grass AM8) and oscilloscope (Tektronix). Isolated activity was captured using CED Spike 2 software. Neural activity was evoked by application of tactile stimuli (brush, finger or Von Frey hairs). Microlesions (10-25 sec, 0.5mA) were made at the termination of several

penetrations on both sides. The location of pV revealed by recording was then used to make a 0.1 μl injection of 10% BDA into the rostral end of the nucleus using a 1.0 μl Hamilton syringe. This animal also received injections of the levator and superior rectus muscles, as described above.

Oculomotor nucleus injections

In order to label the source of afferents supplying the III and CC, we injected 2.0% WGA-HRP into this nucleus (n=2). We approached the brainstem as described above for stereotaxic injections of pV, but placed the aspiration site further rostral, to reveal the surface of the superior colliculus and caudal pole of the thalamus. We then carefully aspirated the cortex immediately in front of the pineal gland, which lies over the midline between the rostral pole of the two sides of the midbrain tectum. At this midline point, we inserted a 1.0 μl Hamilton syringe containing the 2.0% WGA-HRP that had been insulated, except at the tip. We advanced the needle to reach the area of III based on stereotaxic coordinates and measurements of in-house material (Paxinos et al., 2000). There we used microstimulation to produce movements of the eyes and confirm the placement of the syringe needle tip. An AM System isolated pulse stimulator (Model 2100) and a WPI stimulus isolation unit (Model A320) were used to produce stimulus trains [Burst width = 2.5-5.0 ms; interpulse time = 50-150 μs; square wave pulse duration = 25-75 μs, stimulus current = 1-4 mA]. Once the area producing eye movements had been located, we injected 0.01-0.02 μl of the WGA-HRP solution. These animals survived for 2 days for retrograde tracer transport.

Perfusion & Tissue Preparation

In all cases, animals were sedated with ketamine HCl (10 mg/kg, IM) and then deeply anesthetized with sodium pentobarbital (50 mg/kg, IP) at the end of the survival period. They were then perfused through the heart. A peristaltic pump (Masterflex L/S) was used to inject a prewash consisting of buffered saline [0.85 % NaCl in 0.1M, pH 7.2 phosphate buffer (PB)], followed by a fixative solution [1.0% paraformaldehyde and 1.25-1.5% glutaraldehyde in 0.1M, pH 7.2 PB]. The brains were then blocked in the frontal plane and postfixed for 3 hours in the same fixative solution at 4°C. They were stored in 0.1 M, pH 7.2 PB at 4°C.

The brainstem was sectioned on a vibratome (Leica VT1000S) at 100 μm. The sections were collected in 0.1 M, pH 7.2 PB. A 1 in 3 series of sections, at a minimum, was reacted to demonstrate the tracers for light microscopy. To demonstrate the presence of HRP, sections were rinsed in 0.1 M, pH 6.0 PB and then placed in 0.1 M, pH 6.0 PB containing 0.25 % ammonium molybdate and 0.005% tetramethylbenzidine free base (TMB). After a 20 minute pre-incubation, 0.3% H_2O_2 was added to produce a 0.0125% solution and initiate the reaction, which proceeded for 3 hours at room temperature, then overnight at 4°C. This produced a blue reaction product that was stabilized in a 5.0% solution of ammonium molybdate in 0.1 M, pH 6.0 PB. In the cases with injections into III, the sections were mounted on gelatin coated slides, counterstained with cresyl violet, dehydrated, cleared and coverslipped at this point. For the dual tracer experiments, the reaction product was protected as follows. Sections were rinsed in 0.1 M, pH 7.2 PB and then were placed in the same buffer with 0.5% diaminobenzidine (DAB). After a 10 minute pre-incubation, the

reaction was initiated by the addition of 0.3% H_2O_2 to make a 0.005% solution and produce a brown reaction product in the labeled motoneurons. Sections were again rinsed in 0.1 M, pH 7.2 PB followed by the same buffer with 0.1% Triton-X-100 in preparation for reaction to reveal the location of BDA labeled axons. They were then incubated overnight at 4°C in 0.1 M, pH 7.2 PB with 0.1% Triton-X-100 that contained 0.2% avidin conjugated horseradish peroxidase (avidin-HRP). Following rinsing in 0.1 M, pH 7.2 PB, the avidin-HRP was visualized by pre-incubation in a 0.5% DAB solution of 0.1 M, pH 7.2 PB containing 0.01% nickel ammonium sulfate and 0.005% cobalt chloride. The reaction was initiated by the addition of 0.3% H_2O_2 to make a 0.005% solution that produced a black reaction product in the labeled axons. These sections were mounted on gelatin coated slides, counterstained with cresyl violet, dehydrated, cleared and coverslipped. In one animal that just received a BDA injection, only the avidin-HRP protocol was run. In this case, one series was counterstained using the cytochrome oxidase method of Wong-Riley (Wong-Riley, 1989).

In two of the dual tracer experiments, a second series was reacted to demonstrate the presence of the WGA-HRP and BDA tracers for electron microscopic (EM) analysis. The reaction steps differed only in that 0.005% Triton-X-100 was used. The CC was then visualized in free floating sections using a Wild M8 stereoscope and excised. This tissue underwent routine EM processing (Barnerssoi and May, 2016) including osmication, *en bloc* staining with 5.0% uranyl acetate, and embedding in TAAB epoxy 812 resin. Sections were cut on a Reichert-Jung Ultracut E. Semithin sections stained with toluidine blue were used to guide trimming blocks to just include CC. Ultrathin sections were collected on copper grids and stained with lead citrate. These sections were analyzed using a Zeiss EM 10C electron microscope.

Analysis

Low magnification illustrations of sections were made using a Wild M8 stereoscope with attached drawing tube. Labeled neurons and axons were charted or illustrated using an Olympus BH-2 microscope with attached drawing tube. Images were recorded using a Nikon Eclipse E600 microscope and attached Nikon DS-Ri1 digital camera, through the use of Nikon Elements software. Images were adjusted with respect to contrast, brightness and hue to match the appearance of the tissue to the eye when viewed through the microscope by using Adobe Photoshop, which was also used to assemble the final figures.

RESULTS

Trigeminal Injection Cases

An example case (Case 1) with a small BDA injection into the left pV is shown in figure 1. The injection site was centered in pV (Fig. 1j-k) and extended slightly rostral to this nucleus (Fig. 1i). Spread of tracer up the needle track involved the lateral edge of the parabrachial nuclei and the medial edge of the middle cerebellar peduncle (Fig. 1j). BDA labeled axon terminal arbors (stipple) were observed bilaterally in CC and in the supraoculomotor area (SOA) that surrounds it (Fig. 1e-h), with no obvious side preference. They were also present more rostrally in the SOA (Fig. 1c-d), but not all the way to its rostral pole (Fig. 1a-b).

Within CC, the distribution of BDA labeled terminal arbors overlapped with the bilateral distribution of retrogradely labeled motoneurons (red dots) produced by an injection of the right levator muscle (Fig. 1e-h). In this case, the right superior rectus muscle was also injected with WGA-HRP, retrogradely labeling motoneurons primarily in III on the left (Fig. 1b-g). Labeled superior rectus motoneurons were also present in the S-group, sandwiched between the two sides of III (Fig. 1a-e). The S-group motoneurons supply multiply innervated fibers in the superior rectus and inferior oblique muscles (Büttner-Ennever et al., 2001). No BDA labeled axonal arbors were observed within III in this case, and while a few were seen in the area of the S-group (Fig. 1d), they were not associated with the labeled superior rectus motoneurons.

The overlap in the distribution of BDA labeled axonal arbors and WGA-HRP labeled levator motoneurons can be better appreciated in the high magnification illustration shown in figure 2. The numerous BDA labeled axonal arbors extended through CC and around CC in the SOA. These axons were of relatively fine caliber. Boutons on these arbors were often found in close association (arrowheads) with the primary and secondary dendrites of the retrogradely labeled levator motoneurons. Specific examples of the close associations seen in this case (Case 1) are further demonstrated in figure 3a-d. The levator motoneurons extended dendrites into the portion of the SOA that surrounds the lateral (Fig. 3a) and dorsal (Fig. 3b) edge of CC. There they were in close association (arrowheads) with numerous BDA labeled boutons (Fig. 3a-b). Other BDA labeled axonal arbors coursed within CC (Fig. 3c-d), where boutons were also observed making close associations with the labeled motoneurons. Close associations mainly targeted the dendrites of the levator motoneurons (Fig. 3a-d), but occasional axosomatic relationships were also evident (Fig. 3c-d).

While close associations are highly suggestive of synaptic contact, EM examination is needed to prove their presence. As shown in figure 4, the BDA reaction product produced an electron dense staining of the labeled terminals (At*) that were easily differentiated from unlabeled terminals (At). In some cases, this was so dense that it was difficult to make out the profile’s internal structure (Fig. 4c-d), but in others, it just created a fuzzy rim around the vesicles (Fig. 4a-b). When they could be visualized, these clear vesicles displayed a pleomorphic morphology, which is often correlated with inhibitory neurotransmitters. Occasional dense-cored vesicles, suggestive of peptidergic co-transmitters, were also observed in the labeled terminals (Fig. 4a, white arrows). The WGA-HRP reaction product was evident as patches of electron dense crystals (black arrows) in the cytoplasm of labeled dendrites (Den*)(Fig. 4c). Labeled axon terminals were observed in synaptic contact (arrowheads) with both retrogradely labeled (Fig. 4b-d) and unlabeled dendrites (Den)(Fig. 4a). As best demonstrated in figure 4b, these contacts had a symmetric appearance, which is also often correlated with inhibitory action.

The results varied to some extent among the 4 cases with stereotaxic dual tracer injections, most likely due to differences in their injection sites (Fig. 5a-d). Two of the other cases (Fig. 5, Cases 2 and 3) also displayed numerous distinct close associations between BDA labeled axonal boutons and WGA-HRP labeled levator motoneurons. Examples from Case 2 are shown in figure 6a-b. Both axodendritic and axosomatic associations are apparent. In this case, a few terminal arbors were also present in III. These arbors were often organized into

grapelike clusters (Fig. 6c-d), a different arrangement than that seen within CC. In Case 3, in addition to terminals contacting levator motoneurons, we observed a few boutons in close association with superior rectus motoneurons (Fig. 6f). In the fourth case (Fig. 5, Case 4), the injection site was actually centered in pars oralis of the spinal trigeminal nucleus, not pV, and it did not produce labeled axonal arbors in CC. In all the cases where we observed terminal arbors within III proper, there was tracer spread from the needle track that entered the lateral edge of the vestibular complex (Fig. 5c-d, Cases 2-4). The fourth case (Fig. 5, Case 4), with the pars oralis injection, had the greatest involvement of the lateral vestibular nucleus. This case produced very dense labeling in III, but no terminals in close association with the levator motoneurons in CC. In these three cases with vestibular involvement (Fig. 5c-d, Cases 2-4), we also observed labeled axons in the medial longitudinal fasciculus and axons that entered III that were much thicker in caliber (Fig. 6e). In the two additional cases with medial rectus injections (Fig. 5, Cases 2&3), we did not observe close associations with labeled medial rectus motoneurons.

In order to gain a better appreciation of the arrangement of the labeled axonal arbors supplying CC, in one series of sections from with pV injection case (Fig. 5, Case 2), we only reacted the material to visualize the BDA. The result is shown in figure 6g. Fine BDA labeled axons course through the field of faintly labeled levator motoneurons. They branch relatively sparsely, and are studded with *en passant* boutonal enlargements. Similarly, in the case with a large BDA injection that included pV and sVo, where the muscles were not injected (Fig. 5, Case 5), numerous axonal arbors were found in the oculomotor complex. In sections conterstained for cytochrome oxidase, a dense halo of terminals was present in the SOA around the dorsal (Fig. 7a) and lateral (Fig. 7b) edges of the CC. Numerous labeled terminal arbors were also present within CC itself (Fig. 7c-d). Higher magnification views (Fig. 7e-g) again show relatively fine axons (thin arrows) studded with *en passant* boutons in CC (Fig. 7e-f) and in SOA (Fig. 7g). Occasionally, boutons are found on short branches. Within CC, some of the boutons were in close association (arrowhead) with the somata stained for cytochrome oxidase (Fig. 7e-f). This larger injection site also encroached on the vestibular complex (Fig. 5, Case 5). Labeled axons were present in the medial longitudinal fasciculus, and thicker axons produced arbors within III. A few of these (thick arrows) were present in the CC as well (Fig. 7e).

Physiologically Directed Trigeminal Injection

In one awake behaving monkey, we examined the neuronal activity in pV before making an injection. Based on electrode track reconstructions and microlesions, we observed an ordered topography of face representations within pV (Fig. 8a). Receptive fields belonging to the mandibular division of the nerve that were located on the right jaw and lower lip were found dorsally in the right pV (Fig. $8a_{1\text{-}2}$). Those belonging to the maxillary division that were located on the upper lip and infraorbital area were located in the middle of the nucleus (Fig. $8a_{3\text{-}4}$). Those that travel in the ophthalmic division, including receptive fields on the upper eyelid, were found ventrally in the nucleus (Fig. $8a_{5\text{-}6}$). We paid close attention to stimulation sites that might be likely to elicit a blink response. The example shown in figure 8b was a unit that responded to bending a guard hair on the cheek. This was a fast adapting unit that displayed a burst of spikes at the initiation of the hair movement and when the hair

was released. No spikes were present in the interim, while the hair was bent, no matter how long this period lasted (Fig. 8b_{1-4}). The example response shown in figure 8c is from a unit that responded to brushing the eyebrow hairs in either direction. This neuron responded in a one to one manner to stimuli delivered at a brisk pace. A similar response was seen in a unit that received input from the skin just beneath the orbit, when it was touched with a von Frey hair.

Following characterization of the receptive field properties in pV and pars oralis of the spinal trigeminal nucleus on both sides, we injected BDA into the right pV. The reconstructed electrode tracks are shown in figure 9c-e. The BDA injection site (Fig. 5, Case 6) involved the dorsal portion of pV (Fig. 9c), and spread rostrally from there to involve the middle cerebellar peduncle and the lateral edge of the pontine reticular formation (Fig. 9a-b). This injection produced labeled terminals in the dorsal subdivision of the ipsilateral facial nucleus, where orbicularis oculi motoneurons are located (Fig. 9c-d). It also labeled axonal arbors bilaterally in the SOA and CC (Fig. 9a_1). The number of labeled axons in the CC and SOA was not as great as that seen with some of the stereotaxic injections (Figs. 1-3). This animal also had WGA-HRP injected into the right levator muscle and superior rectus muscle, which retrogradely labeled motoneurons (dots) in CC and III, respectively (Fig. 9a_1). In this case (Fig. 5, Case 6), where there was no spread into the vestibular nuclei, no labeled terminal arbors were observed within III or in association with labeled superior rectus motoneurons. As shown in the higher magnification illustration (Fig. 10), a number of close association (arrowheads) were observed between BDA labeled boutons and the dendrites of retrogradely labeled levator motoneurons. These were found both within the CC and on dendrites that extended into the SOA. Other examples of these axodendritic associations are presented in figure 6h.

Oculomotor Complex Injections

In order to identify the likely source of the terminal arbors observed in the CC and SOA, we placed retrograde tracer in the oculomotor complex. In the example shown in figure 11, the injection site includes III on both sides and the SOA dorsal to it (Fig. 11b-d), as well as CC (Fig. 11c). Ventrally, it extended into the MLF and dorsally it extended into the periaqueductal gray between the SOA and cerebral aqueduct. Numerous retrogradely labeled cells (dots) were observed in the known sources of afferents to III and CC. These included: the rostral interstitial nucleus of the medial longitudinal fasciculus (riMLF) and the adjacent M-group (Fig. 11a), the interstitial nucleus of Cajal (InC) (Fig. 11b), the central mesencephalic reticular formation (cMRF) (Fig. 11c-e), the vestibular nuclei (Fig. 11h-i), the abducens nucleus (Fig. 11h) and the pontine reticular formation (PRF) (Fig. 11g-i). Only an occasional labeled cell was observed in the spinal trigeminal nuclei (Fig. 11h). However, a dorsoventrally arranged set of retrogradely labeled neurons was found immediately rostral to pV (Fig. 11e-f). The distribution of these cells located rostral to pV (boxes, Fig. 11e-f) is presented in greater detail in figure 12. Most of these cells lay just medial to the medial edge of the exiting bundles of the trigeminal nerve and the medial border of the middle cerebellar peduncle, in a narrow zone located at the lateral edge of the pontine reticular formation. This relationship to the bundles of the fifth cranial nerve is also evident in the photomicrographic

plates (Fig. 13a,c). The labeled neurons were quite small with long axes ranging between 9-14 μm (Fig. 13b,d).

DISCUSSION

The results of this study clearly indicate the presence of a projection from cells lining the rostral edge of the principal trigeminal sensory nucleus to the levator palpebrae superioris motoneurons located in the caudal central subdivision of the oculomotor complex (Fig. 14, red circuit). This projection directly synapses on these motoneurons. These results represent the first, to the best of our knowledge, examination of this pathway in a primate. A similar projection in the cat was demonstrated to be inhibitory and have relatively slowly conducting axons (May et al., 2012). The ultrastructure of the labeled synapses observed in the present study and the relatively small diameter of the cells of origin for this projection in the macaque support the likelihood that this is also true of the monkey pathway. Considering the location of the cells of origin in the macaque, and the data from the previous cat study (May et al., 2012), we believe the most likely function of this pathway is to suppress the tonic activity of levator motoneurons when the trigeminal system triggers the closing phase of a blink. The projection is bilateral, as is the distribution of levator motoneurons, suggesting that it supports bilateral closure of the eyelids during a blink. In addition, based on the fact that labeled terminal arbors were not present in the oculomotor nucleus proper when the injection sites did not involve the vestibular nuclei, we conclude that this pathway is not used to activate the rectus muscles in order to retract the globe during a blink.

Technical Considerations

All of the BDA injections that included pV and the area immediately rostral to it produced labeled terminals in CC, strongly supporting the presence of a projection to the levator motoneurons (Fig. 5, Cases 1-3 & 5-6). However, none of the BDA injections made in this study were confined to pV. They variously spread into the middle cerebellar peduncle, adjacent pontine reticular formation, parabrachial nuclei and the lateral and superior vestibular nuclei. A control injection in the peduncle did not label this pathway (Fig. 5, Case 7), eliminating the concern that cerebellar axons were labeled in passing. Cells were retrogradely labeled in the parabrachial nuclei after injections of III, however, they were medially located, outside of the area that the BDA injections infringed upon (Fig. 11f-g). In addition, the case shown in figure 9, did not significantly involve the parabrachial nuclei, but still labeled terminal arbors in CC. So it seems unlikely that spread into the parabrachial nucleus was a contributor to the labeling seen in the CC. The retrograde component of the study suggests that the pontine reticular formation is the source of projections to the oculomotor complex (Fig. 11g-h). However, these labeled cells were not found in the immediate vicinity of pV. Moreover, the two illustrated cases (Fig. 1 & 9) only involved a small region of pontine reticular formation immediately adjacent to pV. So we do not believe that reticular projections are responsible for the labeled terminals observed in CC. This is a noteworthy finding, as the paratrigeminal reticular formation in the pons (Fig. 14) has been implicated in activating both orbicularis oculi motoneurons and retractor bulbi motoneurons during trigeminally elicited blinks (cat: Holstege et al., 1986; 1988; rabbit: van Ham and Yeo, 1996; macaque: May and Warren, 2021). It appears that the pontine portion of this

paratrigeminal region is solely responsible for the excitatory components of the blink closing phase, and that the inhibitory circuits supplying III are instead located in the region lining the rostral edge of pV.

It is likely that spread into the vestibular nuclei produced labeled axon terminals in both III and CC in several of our cases. However, the fact that the two cases which did not involve these nuclei (Fig. 5, Case 1 & 6; Fig. 1 & 9) still produced labeled CC terminals, strongly supports our contention that the cells lining the rostral edge of pV are the main source of the blink-related projection. We also saw morphological differences when tracer spread into the vestibular complex, including labeled axons in the medial longitudinal fasciculus, thicker caliber labeled axons and the presence of axonal arbors arranged in grape-like clusters in III. These characteristics increased when there was greater involvement of the vestibular nuclei, and they matched those seen in studies of vestibular projections (McCrea et al., 1987), so we concluded that vestibular neurons, not cells at the rostral border of pV, are the source of the axonal arbors observed in III.

The WGA-HRP injection into the oculomotor complex included III, CC, and the SOA; regions where terminal fields were observed in the BDA injection cases. However, there was also spread into the periaqueductal gray above the SOA and into the medial longitudinal fasciculus and immediately adjoining gray matter. In addition, the preganglionic Edinger-Westphal nucleus (EWpg), which lies within the SOA, was involved. So not all of the cells that were retrogradely labeled following this injection may supply III and CC. For example, labeling in the periaqueductal gray caudal to the injection site (Fig. 11f-g) is likely due to interconnections within the periaqueductal gray, and labeling of cells in the olivary pretectal nucleus is likely due to projections to the EWpg (May & Warren, 2020). However, most of the retrograde labeling was found in known afferents to the motoneurons in III. The retrograde results on their own, cannot identify the source of the input to the CC, but comparison of the anterograde and retrograde results strongly suggests that it is the retrogradely labeled neurons lining the rostral edge of pV.

Comparison to Previous Studies

Cells in the vicinity of pV have been labeled retrogradely in previous studies of oculomotor nucleus afferents. They were first described by Graybiel and Hartwieg (1974) in the cat. A more detailed description of their location in the cat indicated that they lined the rostral and ventral edge of pV, and were often found in association with the fiber bundles of the trigeminal and facial nerves (May et al., 2012). In the rabbit, labeled cells were observed rostral to pV and between the motor trigeminal nucleus and pV (Guerra-Seijas et al., 1993). In the current macaque study, the cells labeled retrogradely by the injection were located in a very narrow band along the rostral edge of pV, and were only associated with fiber bundles of the trigeminal nerve. These were not reported in a previous retrograde study in the macaque (Steiger and Büttner-Ennever, 1979), but might have been easily overlooked in a survey of oculomotor afferents due to their very limited distribution.

Anterograde studies also support a projection from pV to the oculomotor complex. In the rabbit, anterogradely labeled fibers were found in III, within the regions containing the motor pools for the superior rectus muscle, medially, and the levator muscle, laterally

(Guerra-Seijas et al., 1993). The authors suggested this pathway coordinated levator and eye movements during blinks. A second rabbit anterograde study indicated that terminal fields from both pV and pars oralis of the spinal trigeminal nucleus primarily terminate along the dorsal edge of III and the adjacent SOA. They were adjacent to, but did not overlap with the distribution of levator motoneurons (van Ham and Yeo, 1996). In the cat, a projection to the SOA was first reported following an injection that included pV (Ogasawara, 1985). The function proposed for this projection was production of Bell's phenomenon, where the eyes roll upwards with lid closure. A second study in cats indicated that the primary target of this projection was levator motoneurons, but could not eliminate the possibility that rectus motoneurons were also targeted (May et al., 2012). The present study suggests that just levator motoneurons are targeted in macaque monkeys.

In the Results, we did not specify the nucleus within which we found the retrogradely labeled neurons following injections of III (Fig. 12-13). In the frontal plane, pV ends fairly abruptly, making it difficult to say whether this vertically oriented population lies within, or just rostral to pV. This point relates to a larger question of whether these cells receive monosynaptic input from trigeminal primary afferents. In the cat, the distribution of anterogradely labeled ophthalmic division terminals was observed to overlap with the distribution of the cells projecting to III, suggesting a monosynaptic connection (May et al., 2012). However, the physiological evidence presented in this same study was equivocal on this point. While trigeminal primary afferent terminal fields are present at the most rostral levels of pV illustrated in previous macaque studies (Marfurt and Echtenkamp, 1988; May and Porter, 1998), it is difficult to assess whether they overlapped with the cells observed projecting to III here. Determining whether these levator motoneuron afferents receive monosynaptic trigeminal primary afferent input in the primate will require further anatomical and physiological investigation.

Functional Implications

We did not observe a projection to rectus motoneurons in III following pV injections unless the injection site involved the vestibular nuclei. We interpreted this pattern as indicating that the cells lining the rostral edge of pV are primarily targeting levator motoneurons, and inhibiting them during the closing phase of a blink. Based on this interpretation, the excitatory drive to rectus motoneurons that pull the globe into the orbit during a blink must be supplied from some other, as yet undefined, source. This may be reasonable, as it would separate blink-related excitatory and inhibitory populations, allowing them to be more easily regulated by independent means.

In the present study, afferents to the oculomotor complex were observed in the vertical gaze centers (Fig. 11). It has been suggested that blink-related activation of the rectus muscles might utilize gaze circuitry, as omnipause stimulation inhibits blinks (Mays and Morrisse, 1995) and the vertical recti appear to be particularly involved in retraction (Bour et al., 2000; Bergamin et al., 2002, although see Evinger & Manning, 1993). However, the suppression of omnipause activity is poorly correlated with the kinematics of these eye movements, and gaze circuitry is generally organized to produce coordination of agonists and antagonists, not co-contraction, as is needed here (Gnadt et al., 1997; Schultz et al., 2010). So it may be more

likely that this eye retraction drive originates from a brainstem blink center. We did observe retrogradely labeled neurons in the caudal pontine and rostral medullary reticular formation, but not in the spinal trigeminal nucleus (Fig. 11). Consequently, we examined cases in our collection with BDA injections involving the reticular formation of the caudal brainstem (May and Warren, 2021). A portion of those which produced terminal fields in the facial nucleus also displayed labeled axonal arbors in III (not illustrated). This putative pathway from the medullary portion of the paratrigeminal reticular formation, which is illustrated in brown in the summary diagram (Fig. 14), should be targeted for future investigation.

The function of the projection to SOA observed here (Fig. 1) also merits consideration. Most of the labeled terminals were concentrated over the caudal pole of III. The distal dendrites of levator motoneurons are known to extend throughout the caudal SOA (cat: May et al., 2012); so the majority of the SOA projection may also target levator motoneurons. There are a number of other possible target populations located within the macaque SOA, including: 1) the medial and inferior rectus motoneurons in the C-group that supply multiply innervated muscle fibers (Büttner-Ennever et al., 2001; Erichsen et al., 2014); 2) the dendrites of motoneurons located within the preganglionic Edinger-Westphal nucleus (EWpg) (May et al., 2018); 3) peptidergic neurons belonging to the centrally projecting Edinger-Westphal (EWcp) population (Horn et al., 2008; May et al., 2008); and 4) near response neurons controlling lens accommodation and vergence (Mays, 1984; Judge and Cumming, 1986, Zhang et al., 1992; Das, 2011; May et al., 2018; Pallus et al., 2018). With respect to the first population, the diffuse, caudally heavier distribution of these terminals does not match the circumscribed location of the C-group, and we did not observe contacts in this study. Furthermore, there is no functional reason to suspect a trigeminal input to these motoneurons. In fact, multiply innervated fibers are believed to have a more tonic role in regulating eye position (Spencer and Porter, 2006; Büttner-Ennever, 2006; but see Hernández et al., 2019), in contradistinction to the phasic withdrawal of the eyes during a blink. With regard to preganglionic motoneurons in EWpg, painful sensory stimulation can cause dilation of the eye. This is mainly due to activation of sympathetic pathways to the dilator pupillae muscle, but it is possible that the projection to the SOA could be inhibiting pupillary preganglionic motoneurons. The peptidergic EWcp population projects widely within the brain, and is believed to play a role in eating and drinking behavior (Weitemeir & Ryabinin, 2005; Kozicz et al., 2011). An input to EWcp from cells conveying trigeminal sensory information from intraoral regions might be expected. However, the distribution of EWcp cells is, if anything, denser rostrally, than caudally, arguing against their being a primary target of the pV projection. Finally, the distribution of lens accommodation-related premotor neurons, presumed to be near response cells, is greatest in the caudal SOA (May et al., 2018), matching the terminal distribution seen here. However, a rationale for a trigeminal input to these cells is not readily apparent.

The numerous labeled terminal boutons in CC following pV injections of BDA (Fig.1), the close associations between these labeled boutons and retrogradely labeled levator motoneurons (Figs 2-3,6,10), and the ultrastructural evidence these represent monosynaptic connections (Fig. 4) strongly support our conclusion that this is a direct trigemino-oculomotor pathway targeting levator motoneurons. Considering the similar findings in the cat, where an inhibitory trigeminal input has been demonstrated (May et al., 2012), we

believe the most parsimonious explanation is that this pathway contributes to the inhibition of levator motoneurons observed during the closing phase of blinks initiated by trigeminal stimulation (Fuchs et al., 1992). This projection may be GABAergic, given that GABA positive neurons are common in and adjacent to pV in the rabbit (Kolta et al., 2000). This inhibition is necessary for the unencumbered action of the orbicularis oculi muscle, which closes the eye very swiftly to protect the cornea. Whether this inhibitory pathway also takes part in suppressing levator activity when the eyes are closed during sleep is unknown. Perhaps not, as activity in many other motoneurons are also suppressed during sleep.

The other noteworthy feature of the projection described here is its bilateral distribution. This matches the fairly balanced bilateral primate distribution of levator motoneurons (Porter et al., 1989), and the fact that some motoneurons may even project to both eyes (Jamilah et al., 1992; VanderWerf et al., 1997; present data). Both these features would argue for bilateral inhibition of levator motoneurons and suppression of the levator muscle activity in response to unilateral trigeminal stimulation. The trigeminal blink reflex is generally elicited by supraorbital nerve stimulation. In rodents, the fastest component of the reflex (R_1) is bilateral (Pelligrini et al., 1995). However, in humans, the R_1 is just ipsilateral at threshold, and it only becomes bilateral at higher stimulation levels (Aramideh & Ongerbour de Visser, 2002), although there is evidence that the lack of a contralateral R_1 response in humans may be due to suppression of facial motoneuron activity (Willer et al., 1984). To the best of our knowledge, the supraorbital blink reflex has not been investigated in the macaque. So we do not have monkey-specific data on whether levator muscles are bilaterally inhibited following unilateral supraorbital stimulation. However, in humans with facial palsy that inactivates the orbicularis oculi muscle, the eyelid is still lowered bilaterally in response to corneal air puffs or supraorbital stimulation (Schicatano et al., 2002; Vanderwerf et al., 2007). This downward motion is produced by relaxing the levators, which releases the tension in the check ligaments of the eyelids, pulling them downward (Evinger et al., 1991; Sibony et al., 1991). We previously showed that cells within pV and in the adjacent paratrigeminal reticular formation in the macaque do, in fact, provide a monosynaptic input to orbicularis oculi motoneurons in the contralateral facial nucleus (Fig. 14, light and dark blue circuits, respectively)(May and Warren, 2021). So both the excitatory and inhibitory paths are bilateral and direct. However, the cells of origin of the projection to the facial nuclei are not located at the same sites as where trigemino-oculomotor cells were found in the present study (Fig. 14, red circuits). The former lie within pV and the latter line its rostral edge. So it appears that the sources of excitation that bilaterally activate orbicularis oculi motoneurons, and the sources of inhibition that bilaterally suppress levator motoneurons during a blink are segregated within the pons. It is interesting that trigeminal projections to both these motoneuron populations are either monosynaptic or disynaptic, considering levator muscle inhibition actually precedes orbicularis oculi muscle activation (Bjork & Kugelberg, 1953; Manning & Evinger, 1986). The differences in latency must either be due to the shorter pathway between the motor nucleus and its target in the case of III, or to differences in the capacity of these motoneuron populations to be activated. Future studies may reveal how the activity of these two motoneuron populations is coordinated.

Acknowledgements:

We would like to thank the technicians who have assisted us in surgeries, undertaken the histological processing and provided assistance with illustrations for this work: Jayne Bernanke, Olga Golanov, Jennifer Cotton and Jinrong Wei. We are also beholden to Glen Hoskins for his preparation of the EM samples. The work is better for the comments of Dr. Yoshiko Kojima on an earlier draft.

Grant support:

This work was supported by NEI grant EY09762 to PJM, EY014263 to PJM & SW, and a grant from the Benign Essential Blepharospasm Research Foundation to SW & PJM.

ABBREVIATIONS

3n	oculomotor nerve
5n	trigeminal nerve
7n	facial nerve
III	oculomotor nucleus
IV	trochlear nucleus
VI	abducens nucleus
VII	facial nucleus
At	axon terminal
At*	BDA labeled axon terminal
BC	brachium conjunctivum
BDA	biotinylated dextran amine
CC	caudal central subdivision of III
cMRF	central mesencephalic reticular formation
Cun	cuneiform nucleus
Den	dendrite
Den*	WGA-HRP labeled dendrite
DR	dorsal raphe
EWpg	preganglionic Edinger-Westphal nucleus
IC	inferior colliculus
InC	interstitial nucleus of Cajal
IO	inferior olive
LG	lateral geniculate nucleus

LV	lateral vestibular nucleus
M	M-group
MCP	middle cerebellar peduncle
MD	medial dorsal nucleus
MdRF	medullary reticular formation
MLF	medial longitudinal fasciculus
MG	medial geniculate nucleus
ms	millisecond
mV	motor trigeminal nucleus
MV	medial vestibular nucleus
nPC	nucleus of PC
OPt	olivary pretectal nucleus
P	pyramid
PB	parabrachial complex
PC	posterior commissure
PH	nucleus prepositus hypoglossi
PN	pontine nuclei
PRF	pontine reticular formation
PTR	paratrigeminal reticular formation
Pul	pulvinar
pV	principal trigeminal nucleus
riMLF	rostral interstitial nucleus of the MLF
SC	superior colliculus
SGI	intermediate gray layer
SN	substantia nigra
SO	superior olive
SOA	supraoculomotor area
Stim	stimulation
SV	superior vestibular nucleus

sV	spinal trigeminal nucleus
sVi	spinal trigeminal nucleus, pars interpolaris
sVo	spinal trigeminal nucleus, pars oralis
V	volt
VP	ventral posterior nucleus
WGA-HRP	wheat germ agglutinin conjugated horseradish peroxidase

CITATIONS

Adamczyk C, Strupp M, Jahn K & Horn AK (2015) Calretinin as a marker for premotor neurons involved in upgaze in human brainstem. Frontiers in Neuroanatomy 9:153. doi: 10.3389/fnana.2015.00153. [PubMed: 26696837]

Ahlfeld J, Mustari M & Horn AK (2011) Sources of calretinin inputs to motoneurons of extraocular muscles involved in upgaze. Annals of the New York Academy of Science 1233:91–9. doi: 10.1111/j.1749-6632.2011.06168.x.

Akagi Y (1978) The localization of the motor neurons innervating the extraocular muscles in the oculomotor nuclei of the cat and rabbit, using horseradish peroxidase. Journal of Comparative Neurology 181:745–61. doi: 10.1002/cne.901810405.

Aramideh M, Eekhof JL, Bour LJ, Koelman JH, Speelman JD & Ongerboer de Visser BW (1995) Electromyography and recovery of the blink reflex in involuntary eyelid closure: a comparative study. Journal of Neurology, Neurosurgery & Psychiatry 58:692–8. doi: 10.1136/jnnp.58.6.692.

Aramideh M & Ongerboer de Visser BW (2002) Brainstem reflexes: electrodiagnostic techniques, physiology, normative data, and clinical applications. Muscle & Nerve 26:14–30. doi: 10.1002/mus.10120. [PubMed: 12115945]

Barnerssoi M & May PJ (2016) Postembedding immunohistochemistry for inhibitory neurotransmitters in conjunction with neuroanatomical tracers. In: Transmission Electron Microscopy Methods for Understanding the Brain; Ed: Van Bockstaele EJ; Neuromethods vol 115, pp 181–203.

Becker W, & Fuchs AF (1988) Lid-eye coordination during vertical gaze changes in man and monkey. Journal of Neurophysiology 60:1227–52. doi: 10.1152/jn.1988.60.4.1227. [PubMed: 3193155]

Bergamin O, Bizzarri S & Straumann D (2002) Ocular torsion during voluntary blinks in humans. Investigative Ophthalmology & Visual Science 43:3438–43. PMID: 12407154 [PubMed: 12407154]

Bjork A & Kugelberg E (1953) The electrical activity of the muscles of the eye and eyelids in various positions and during movement. Electroencephalography & Clinical Neurophysiology 5:595–602. doi: 10.1016/0013-4694(53)90037-6. [PubMed: 13107607]

Boghen D (1997) Apraxia of lid opening: a review. Neurology 48:1491–4. doi: 10.1212/wnl.48.6.1491. [PubMed: 9191752]

Bour LJ, Aramideh M & de Visser BW (2000) Neurophysiological aspects of eye and eyelid movements during blinking in humans. Journal of Neurophysiology 83:166–76. doi: 10.1152/jn.2000.83.1.166. [PubMed: 10634863]

Büttner-Ennever JA (2006) The extraocular motor nuclei: organization and functional neuroanatomy. Progress in Brain Research 151:95–125. doi: 10.1016/S0079-6123(05)51004-5. [PubMed: 16221587]

Büttner-Ennever JA, Horn AK, Scherberger H & D'Ascanio P (2001) Motoneurons of twitch and nontwitch extraocular muscle fibers in the abducens, trochlear, and oculomotor nuclei of monkeys. Journal of Comparative Neurology 438:318–35. doi:10.1002/cne.1318.

Che Ngwa E, Zeeh C, Messoudi A, Büttner-Ennever JA & Horn AKE (2014) Delineation of motoneuron subgroups supplying individual eye muscles in the human oculomotor nucleus. Frontiers in Neuroanatomy 8:2. doi: 10.3389/fnana.2014.00002. [PubMed: 24574976]

Chen B & May PJ (2002) Premotor circuits controlling eyelid movements in conjunction with vertical saccades in the cat: I. The rostral interstitial nucleus of the medial longitudinal fasciculus. Journal of Comparative Neurology 450:183–202. doi: 10.1002/cne.10313.

Chen B & May PJ (2007) Premotor circuits controlling eyelid movements in conjunction with vertical saccades in the cat: II. Interstitial nucleus of Cajal. Journal of Comparative Neurology 500:676–92. doi: 10.1002/cne.21203.

Das VE (2011) Cells in the supraoculomotor area in monkeys with strabismus show activity related to the strabismus angle. Annals of the New York Academy of Science 1233:85–90. doi: 10.1111/j.1749-6632.2011.06146.x.

Defazio G, Livrea P, Lamberti P, De Salvia R, Laddomada G, Giorelli M & Ferrari E (1998) Isolated so-called apraxia of eyelid opening: report of 10 cases and a review of the literature. European Neurology 39:204–10. doi: 10.1159/000007935. [PubMed: 9635470]

Erichsen JT, Wright NF & May PJ (2014) Morphology and ultrastructure of medial rectus subgroup motoneurons in the macaque monkey. Journal of Comparative Neurology 522:626–41. doi: 10.1002/cne.23437.

Evinger C, Manning KA & Sibony PA (1991) Eyelid movements. Mechanisms and normal data. Investigative Ophthalmology & Visual Science 32:387–400. [PubMed: 1993591]

PMID: 1993591Evinger C & Manning KA (1993) Pattern of extraocular muscle activation during reflex blinking. Experimental Brain Research 92:502–6. doi: 10.1007/BF00229039. [PubMed: 8454013]

Fuchs AF, Becker W, Ling L, Langer TP & Kaneko CR (1992) Discharge patterns of levator palpebrae superioris motoneurons during vertical lid and eye movements in the monkey. Journal of Neurophysiology 68:233–43. doi: 10.1152/jn.1992.68.1.233. [PubMed: 1517822]

Glicksman MA (1980) Localization of motoneurons controlling the extraocular muscles of the rat. Brain Research 188:53–62. doi: 10.1016/0006-8993(80)90556-9. [PubMed: 7370761]

Gnadt JW, Lu SM, Breznen B, Basso MA, Henriquez VM & Evinger C (1997) Influence of the superior colliculus on the primate blink reflex. Experimental Brain Research 116:389–98. doi: 10.1007/pl00005767. [PubMed: 9372288]

Gomez Segade LA & Labandeira Garcia JL (1983) Location and quantitative analysis of the motoneurons innervating the extraocular muscles of the guinea-pig, using horseradish peroxidase (HRP) and double or triple labelling with fluorescent substances. Journal für Hirnforschung 24:613–26. PMID: 6672094 [PubMed: 6672094]

Graybiel AM & Hartwieg EA (1974) Some afferent connections of the oculomotor complex in the cat: an experimental study with tracer techniques. Brain Research 81:543–51. doi: 10.1016/0006-8993(74)90850-6. [PubMed: 4434207]

Gruart A & Delgado-García JM (1994) Discharge of identified deep cerebellar nuclei neurons related to eye blinks in the alert cat. Neuroscience 61:665–81. doi: 10.1016/0306-4522(94)90443-x. [PubMed: 7969937]

Guerra-Seijas MJ, Labandeira Garcia J, Tobio J & Gonzalez T (1993) Neurons located in the trigeminal sensory complex and the lateral pontine tegmentum project to the oculomotor nucleus in the rabbit. Brain Research 601:1–13. doi: 10.1016/0006-8993(93)91689-p. [PubMed: 8431757]

Guitton D, Simard R & Codere F (1991) Upper eyelid movements measured with a search coil during blinks and vertical saccades. Investigative Ophthalmology & Visual Science 32:3298–305. [PubMed: 1748560]

Hernández RG, Calvo PM, Blumer R, de la Cruz RR & Pastor AM (2019) Functional diversity of motoneurons in the oculomotor system. Proceedings of the National Academy of Science U S A 116(9):3837–3846. doi: 10.1073/pnas.1818524116.

Holstege G, van Ham JJ, Tan J & Graveland GA (1986) Anatomical observations on the afferent projections to the retractor bulbi motoneuronal cell group and other pathways possibly related to the blink reflex in the cat. Brain Research 374:321–34. doi: 10.1016/0006-8993(86)90426-9. [PubMed: 3719341]

Holstege G, Tan J & van Ham JJ, (1988) Anatomic observations on afferent projections of orbicularis oculi and retractor bulbi motoneuronal cell groups and other pathways possibly related to the blink

reflex in the cat. In: Cellular Mechanisms of Conditioning and Behavioral Plasticity Ed: Woody CD, Plenum Publishing Corp., pp 273–286.

Horn AK, Büttner-Ennever JA, Gayde M & Messoudi A (2000) Neuroanatomical identification of mesencephalic premotor neurons coordinating eyelid with upgaze in the monkey and man. Journal of Comparative Neurology 420:19–34. doi: 10.1002/(sici)1096-9861(20000424)420:1<19::aid-cne2>3.0.co;2-d.

Horn AK, Eberhorn A, Härtig W, Ardeleanu P, Messoudi A & Büttner-Ennever JA (2008) Perioculomotor cell groups in monkey and man defined by their histochemical and functional properties: reappraisal of the Edinger-Westphal nucleus. Journal of Comparative Neurology 507:1317–35. doi: 10.1002/cne.21598.

Jamilah J, Myint K & Rajikin MH (1992) Localization, number and size distribution of motoneurons supplying the levator palpebrae superioris muscle in *Macaca fascicularis*. Medical Science Research 20:287–289

Judge SJ & Cumming BG (1986) Neurons in the monkey midbrain with activity related to vergence eye movement and accommodation. Journal of Neurophysiology 55:915–30. doi: 10.1152/jn.1986.55.5.915. [PubMed: 3711972]

Kolta A, Westberg KG & Lund JP (2000) Identification of brainstem interneurons projecting to the trigeminal motor nucleus and adjacent structures in the rabbit. Journal of Chemical Neuroanatomy 19:175–95. doi: 10.1016/s0891-0618(00)00061-2. [PubMed: 10989261]

Kozicz T, Bittencourt JC, May PJ, Reiner A, Gamlin PD, Palkovits M, Horn AK, Toledo CA & Ryabinin AE (2011) The Edinger-Westphal nucleus: a historical, structural, and functional perspective on a dichotomous terminology. Journal of Comparative Neurology 519:1413–34. doi: 10.1002/cne.22580.

Labandeira Garcia JL, Gomez Segade LA & Suarez Nuñez JM (1983) Localization of motoneurons supplying the extra-ocular muscles of the rat using horseradish peroxidase and fluorescent double labelling. Journal of Anatomy 137:247–61. PMID: 6195140 [PubMed: 6195140]

Manning KA & Evinger C (1986) Different forms of blinks and their two-stage control. Experimental Brain Research 64:579–88. doi: 10.1007/BF00340495. [PubMed: 3803493]

Marfurt CF & Echtenkamp SF (1988) Central projections and trigeminal ganglion location of corneal afferent neurons in the monkey, *Macaca fascicularis*. Journal of Comparative Neurology 272:370–82. doi: 10.1002/cne.902720307.

May PJ & Porter JD (1998) The distribution of primary afferent terminals from the eyelids of macaque monkeys. Experimental Brain Research 123:368–81. doi: 10.1007/s002210050582. [PubMed: 9870597]

May PJ & Warren S (2020) Pupillary light reflex circuits in the macaque monkey: the olivary pretectal nucleus. Brain Structure & Function 225:305–320. doi: 10.1007/s00429-019-02003-7. [PubMed: 31848686]

May PJ, Reiner AJ & Ryabinin AE (2008) Comparison of the distributions of urocortin-containing and cholinergic neurons in the perioculomotor midbrain of the cat and macaque. Journal of Comparative Neurology 507:1300–16. doi: 10.1002/cne.21514.

May PJ, Vidal PP, Baker H & Baker R (2012) Physiological and anatomical evidence for an inhibitory trigemino-oculomotor pathway in the cat. Journal of Comparative Neurology 520:2218–40. doi: 10.1002/cne.23039.

May PJ, Warren S, Gamlin PDR & Billig I (2018) An anatomic characterization of the midbrain near response neurons in the macaque monkey. Investigative Ophthalmology & Visual Science 59:1486–1502. doi: 10.1167/iovs.17-23737. [PubMed: 29625471]

May PJ & Warren S (2021) Macaque monkey trigeminal blink reflex circuits targeting orbicularis oculi motoneurons. Journal of Comparative Neurology. doi: 10.1002/cne.25130. Online ahead of print.

Mays LE (1984) Neural control of vergence eye movements: convergence and divergence neurons in midbrain. Journal of Neurophysiology 51:1091–1108. doi: 10.1152/jn.1984.51.5.1091. [PubMed: 6726313]

Mays LE & Morrisse DW (1995) Electrical stimulation of the pontine omnipause area inhibits eye blink. Journal of the American Optometric Association 66:419–22. [PubMed: 7560729]

McCrea RA, Strassman A & Highstein SM (1987) Anatomical and physiological characteristics of vestibular neurons mediating the vertical vestibulo-ocular reflexes of the squirrel monkey. Journal of Comparative Neurology 264:571–94. doi: 10.1002/cne.902640409

Murphy EH, Garone M, Tashayyod D & Baker RB (1986) Innervation of extraocular muscles in the rabbit. Journal of Comparative Neurology 254:78–90. doi: 10.1002/cne.902540107.

Ogasawara K (1985) Neural pathways mediating the corneal blink reflex and Bell's phenomenon in the cat. Neuroscience Research 2:309–20. doi: 10.1016/0168-0102(85)90043-4. [PubMed: 2412194]

Pallus AC, Walton MMG & Mustari MJ (2018) Response of supraoculomotor area neurons during combined saccade-vergence movements. Journal of Neurophysiology 119:585–596. doi: 10.1152/jn.00193.2017. [PubMed: 29142092]

Paxinos G, Huang X-F & Toga AW (2000) The Rhesus Monkey Brain in Stereotaxic Coordinates, Academic Press, San Diego.

Pellegrini JJ, Horn AK & Evinger C (1995) The trigeminally evoked blink reflex. I. Neuronal circuits. Experimental Brain Research 107:166–80. doi: 10.1007/BF00230039. [PubMed: 8773237]

Porter JD, Burns LA & May PJ (1989) Morphological substrate for eyelid movements: innervation and structure of primate levator palpebrae superioris and orbicularis oculi muscles. Journal of Comparative Neurology 287:64–81. doi: 10.1002/cne.902870106.

Porter JD, Stava MW, Gaddie IB & Baker RS (1993) Quantitative analysis of eyelid movement metrics reveals the highly stereotyped nature of monkey blinks. Brain Research 609:159–66. doi: 10.1016/0006-8993(93)90869-o. [PubMed: 8508300]

Schicatano EJ, Mantzouranis J, Peshori KR, Partin J & Evinger C (2002) Lid restraint evokes two types of motor adaptation. Neuroscience 22:569–76. doi: 10.1523/JNEUROSCI.22-02-00569.2002. [PubMed: 11784804]

Schmidtke K & Büttner-Ennever JA (1992) Nervous control of eyelid function. A review of clinical, experimental and pathological data. Brain 115:227–47. doi: 10.1093/brain/115.1.227 [PubMed: 1559156]

Schultz KP, Williams CR & Busettini C (2010) Macaque pontine omnipause neurons play no direct role in the generation of eye blinks. Journal of Neurophysiology 103:2255–74. doi: 10.1152/jn.01150.2009. [PubMed: 20164389]

Sekiya H, Kojima Y, Hiramoto D, Mukuno K & Ishikawa S (1992) Bilateral innervation of the musculus levator palpebrae superioris by single motoneurons in the monkey. Neuroscience Letters 146:10–2. doi: 10.1016/0304-3940(92)90159-5. [PubMed: 1282224]

Sibony PA, Evinger C & Manning KA (1991) Eyelid movements in facial paralysis. Archives of Ophthalmology 109:1555–61. doi: 10.1001/archopht.1991.01080110091043. [PubMed: 1755737]

Spencer RF & Porter JD (2006) Biological organization of the extraocular muscles. Progress in Brain Research 151:43–80. doi: 10.1016/S0079-6123(05)51002-1. [PubMed: 16221585]

Steiger HJ & Büttner-Ennever JA (1979) Oculomotor nucleus afferents in the monkey demonstrated with horseradish peroxidase. Brain Research 160:1–15. doi: 10.1016/0006-8993(79)90596-1. [PubMed: 102412]

Sun W & May PJ (1993) Organization of the extraocular and preganglionic motoneurons supplying the orbit in the lesser galago. Anatomical Record 237:89–103. doi: 10.1002/ar.1092370109.

van Ham JJ & Yeo CH (1996) Trigeminal inputs to eyeblink motoneurons in the rabbit. Experimental Neurology 142:244–57. doi: 10.1006/exnr.1996.0195. [PubMed: 8934557]

VanderWerf F, Aramideh M, Ongerboer de Visser BW, Baljet B, Speelman JD & Otto JA (1997) A retrograde double fluorescent tracing study of the levator palpebrae superioris muscle in the cynomolgus monkey. Experimental Brain Research 113:174–9. doi: 10.1007/BF02454155. [PubMed: 9028788]

VanderWerf F, Reits D, Smit AE & Metselaar M (2007) Blink recovery in patients with Bell's palsy: a neurophysiological and behavioral longitudinal study. Investigative Ophthalmology & Visual Science 48:203–13. doi: 10.1167/iovs.06-0499. [PubMed: 17197534]

Weitemier AZ & Ryabinin AE (2005). Lesions of the Edinger-Westphal nucleus alter food and water consumption. Behavioral Neuroscience 119, 1235–1243. doi: 10.1037/0735-7044.119.5.1235. [PubMed: 16300431]

Willer JC, Boulu P & Bratzlavsky M (1984) Electrophysiological evidence for crossed oligosynaptic trigemino-facial connections in normal man. Journal of Neurology, Neurosurgery & Psychiatry 47:87–90. doi: 10.1136/jnnp.47.1.87.

Wong-Riley MTT (1989) Cytochrome oxidase: an endogenous metabolic marker for neuronal activity. Trends in Neurosciences 12:94–101. [PubMed: 2469224]

Zeeh C, Hess BJ & Horn AK (2013) Calretinin inputs are confined to motoneurons for upward eye movements in monkey. Journal of Comparative Neurology 521:3154–66. doi: 10.1002/cne.23337.

Zhang Y, Mays LE & Gamlin PD (1992) Characteristics of near response cells projecting to the oculomotor nucleus. Journal of Neurophysiology 67:944–60. doi: 10.1152/jn.1992.67.4.944. [PubMed: 1588393]

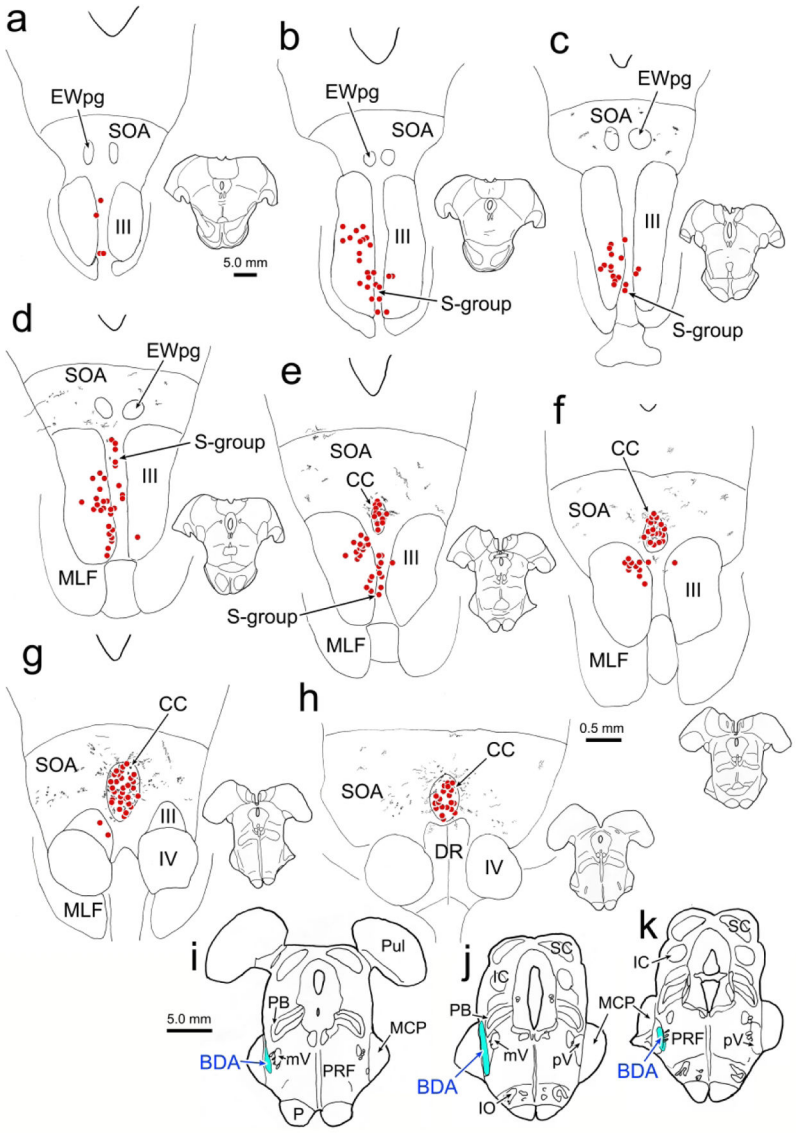

Figure 1.

Relationship of trigeminal projections to the distribution of levator and superior rectus motoneurons. An injection of BDA placed in the left pV (**i-k**) produced anterogradely labeled terminal arbors (stipple) within the SOA and CC (**c-h**). Injections of WGA-HRP into the right superior rectus and levator muscles retrogradely motoneurons (dots) in III (**b-g**), S-group (**a-e**) and CC (**e-h**). Overlap between the labeled terminals and cells was only observed in CC (**e-h**). Note that the charted sections were more closely spaced in **e-h**, to provide greater detail in the area of overlap.

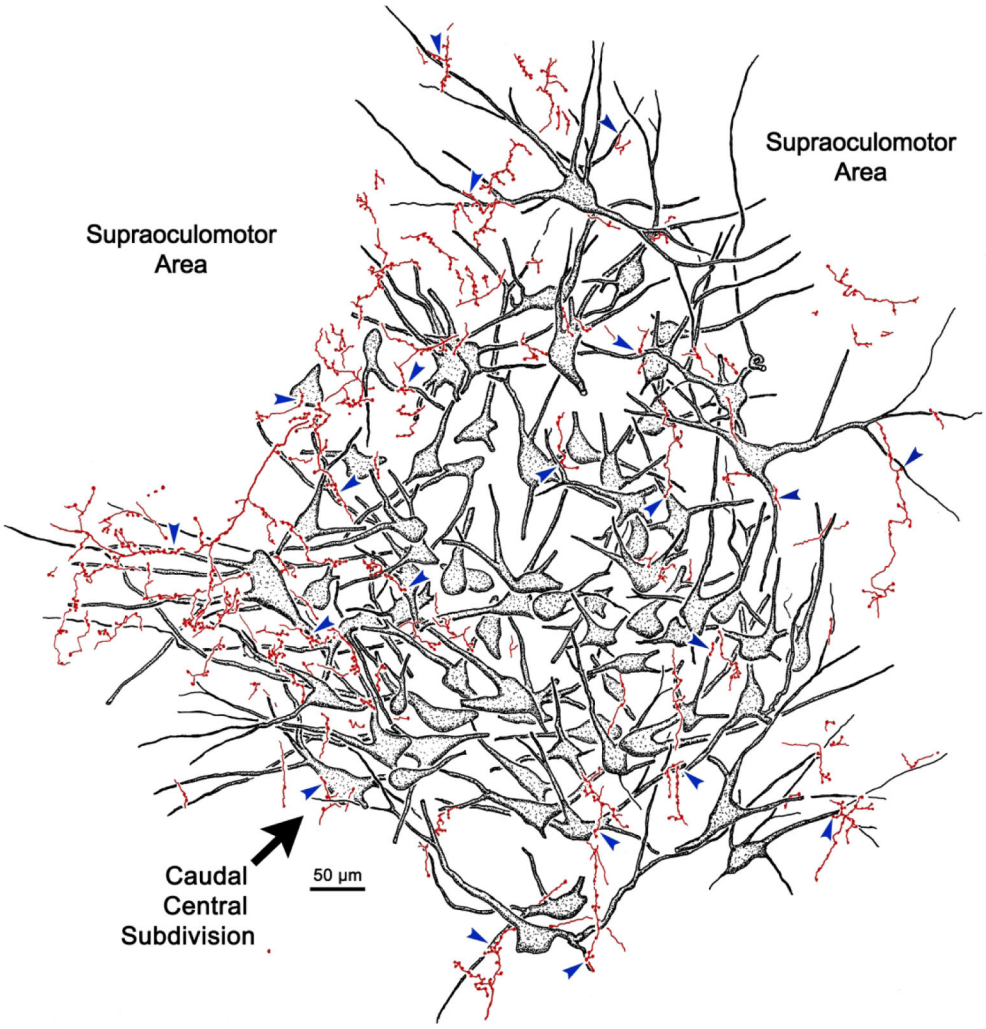

Figure 2.

Close associations between labeled terminal boutons and levator motoneurons. In a higher magnification drawing of CC from the case illustrated in figure 1, retrogradely labeled motoneurons (shaded) are present bilaterally in CC following a unilateral injection of WGA-HRP. Their dendrites extend out into the surrounding SOA. BDA labeled axons are sparsely branched and display numerous *en passant* boutons and occasional terminal boutons. A number of the boutons are in close association (arrowheads) with the dendrites and somata of the levator motoneurons, suggesting synaptic contact.

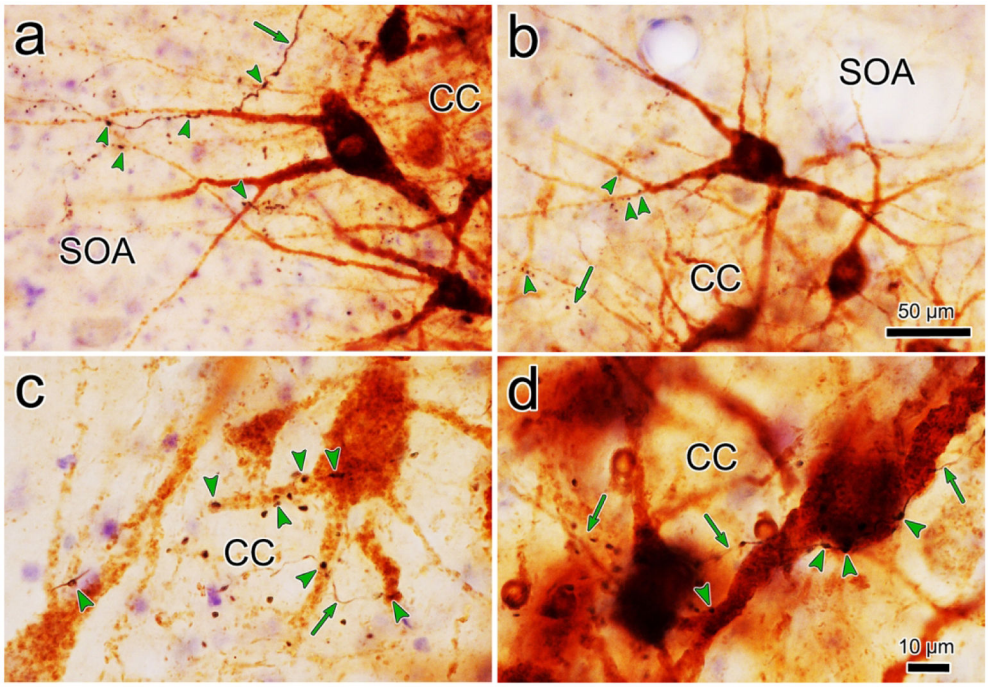

Figure 3.

Relationship of trigeminal boutons to levator motoneurons. Photomicrographs showing the examples of labeling in the case illustrated in figure 1. The dark thin axons (arrows) labeled following a BDA injection of pV display numerous *en passant* and occasional terminal boutons. They arborize in SOA (**a-b**) and within CC (**c-d**). Retrogradely labeled motoneurons (brown) are found within CC and they extend dendrites into SOA. In SOA, the labeled boutons display close associations (arrowheads) with levator motoneuron dendrites. Within CC the close associations target both dendrites and somata. Scale in b=a; d=c.

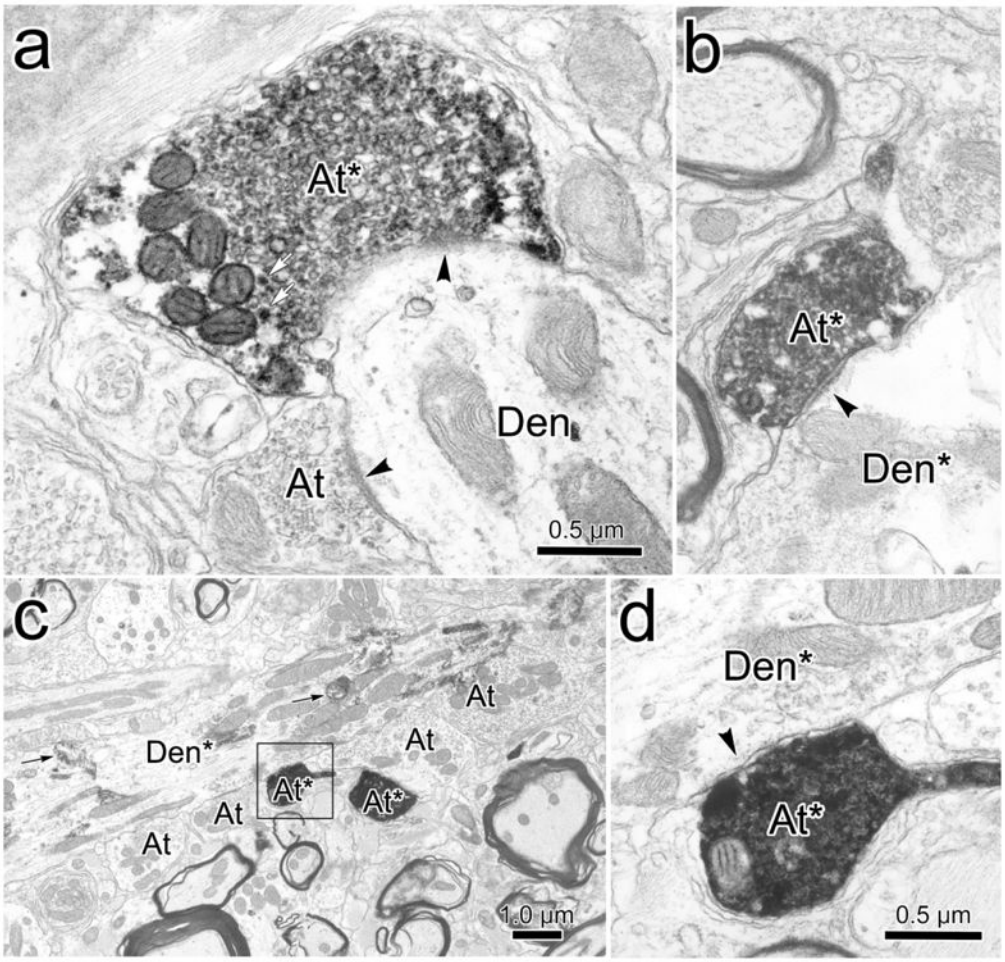

Figure 4.

Monosynaptic relationship between trigeminal terminals and levator motoneurons. BDA labeled axon terminals (At*) observed in CC following injections of pV were electron dense compared to unlabeled axon terminals (At). They contained numerous clear pleomorphic and a few dense-cored vesicles (white arrows, **a**). They made synaptic contacts (arrowhead) with both unlabeled dendrites (Den) (**a**) and retrogradely labeled dendrites (Den*)(**b-d**). The HRP reaction product (black arrows, **c**) consisted of electron dense crystals. The BDA labeled terminals contained pleomorphic vesicles (**a**) and made synapses with symmetric membrane densities (**b**). Scale in d=b.

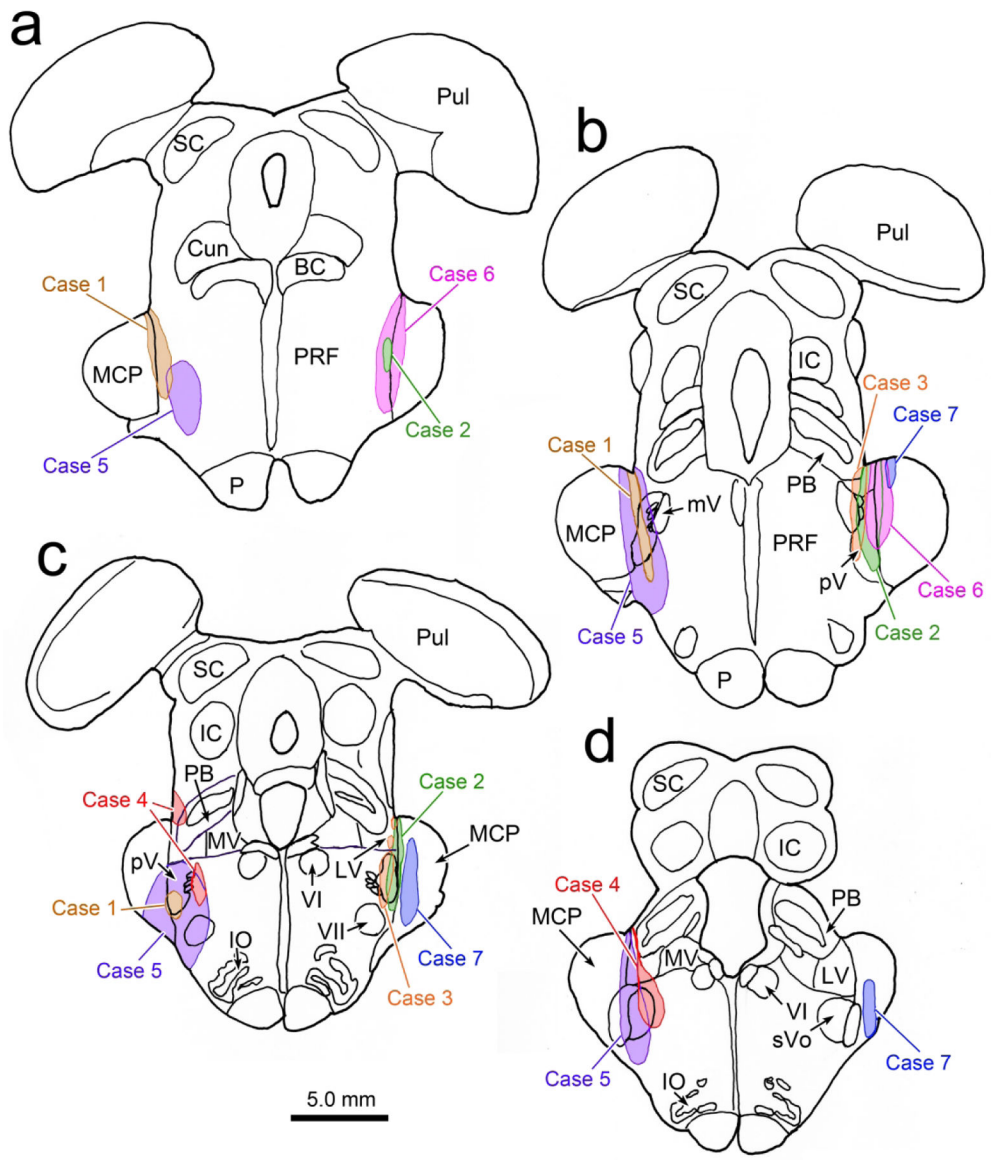

Figure 5.

Injection sites for the trigeminal BDA injections made in this study. For ease of comparison, Cases 2, 3 and 7 are illustrated on the right side, although they were made on the left. The Case 6 injection was on the right. Case 7 is a control injection.

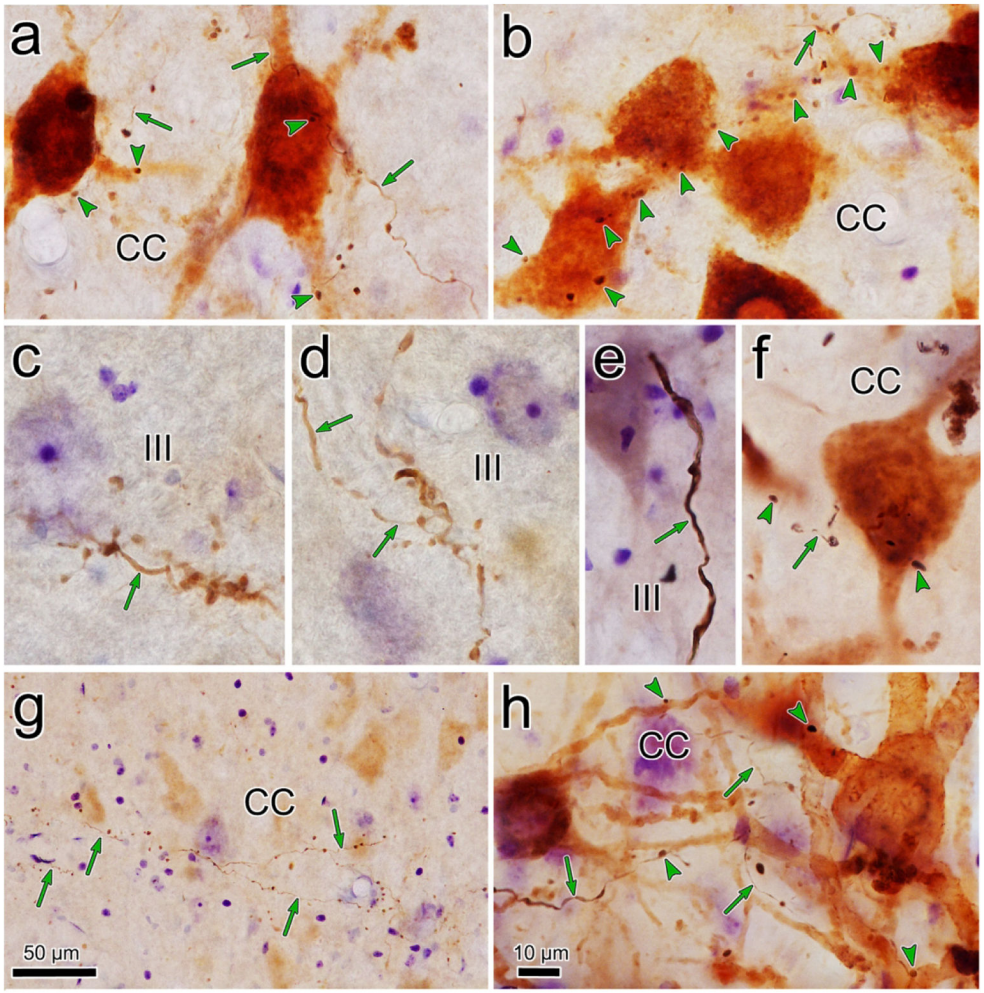

Figure 6.

Comparison of BDA labeled axonal arbors from different cases. **a-b.** Close associations (arrowheads) between BDA labeled axonal boutons and retrogradely labeled levator motoneurons in CC from a case with a pV injection that also involved the vestibular nuclei (Case 2). Most of the labeled axons (arrows) were quite fine in caliber. **c-d.** Examples of BDA labeled axons in III from the same case, showing grape-like organization of axon terminal arbors. **e.** An example of thick BDA labeled axon observed in III when the BDA spread into the vestibular nuclei (Case 5). **f.** Close associations between labeled boutons and labeled superior rectus motoneurons in a case where the pV injection spread into the vestibular nuclei (Case 3). **g.** Morphology of the fine BDA labeled axons in CC. (Case 2, but no reaction performed for WGA-HRP). **h.** Close associations between labeled boutons and labeled motoneurons in the case (Case 6) illustrated in figure 8. Scale in h=a-f.

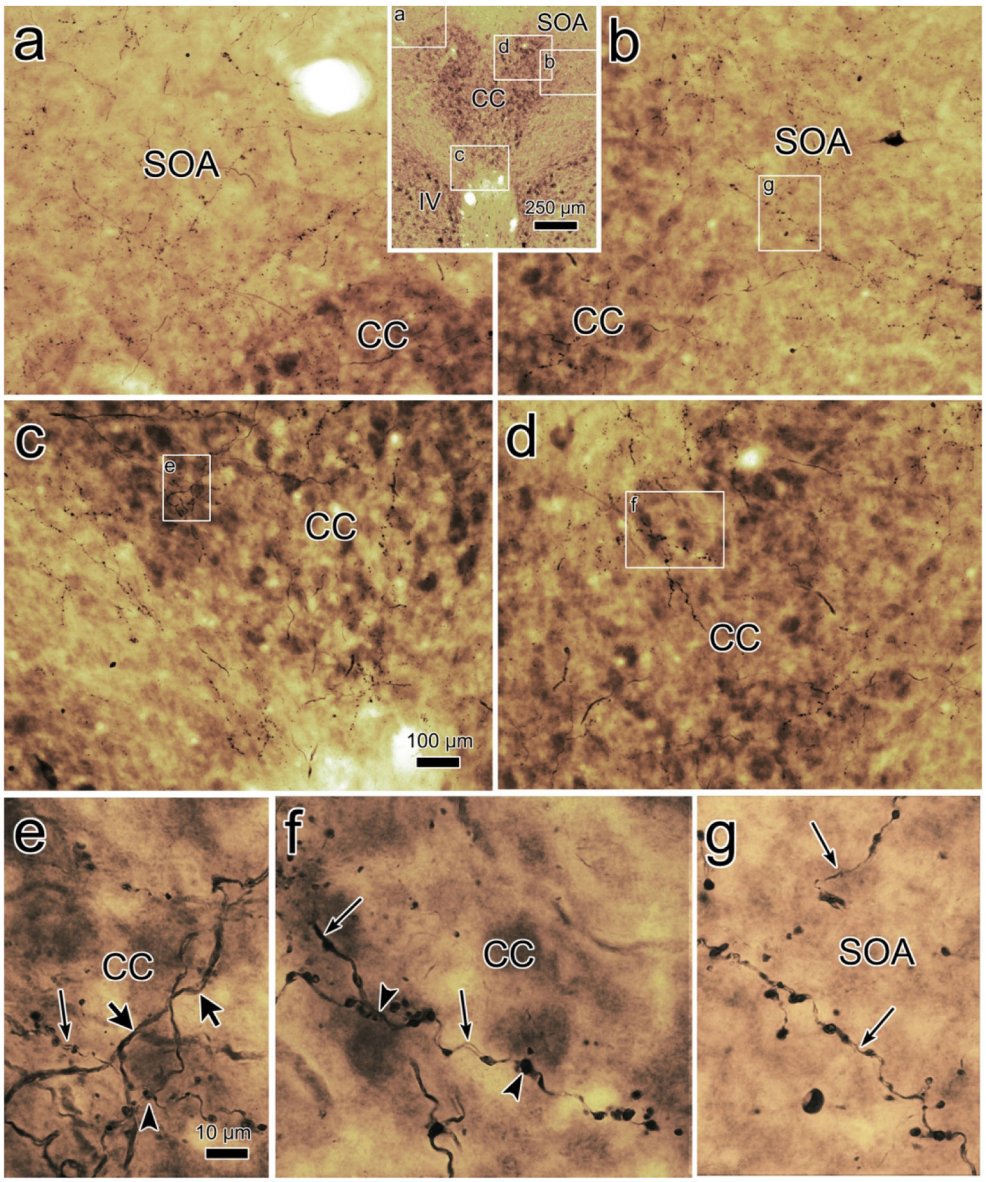

Figure 7.

Morphology of BDA labeled axons in CC and SOA. This case (Case 5) only received a BDA injection in pV on the left, and there was spread into the vestibular nuclei. Sections are counterstained with cytochrome oxidase. Inset, top-middle, indicates location of samples **a-d**. BDA labeled axonal arbors were widespread within the left (**a**) and right (**b**) SOA, as well as within CC on the left (**c**) and right (**d**). Boxed areas in **b, c & d** are shown at higher magnification in **g, e & f**, respectively. **e-f.** Most of the BDA labeled axons (thin arrows) in CC (**e-f**) and the SOA (**g**) were relatively fine in caliber, with numerous *en passant* and occasional terminal boutons. They sometimes made close association with the counterstained somata (arrowheads; **e-f**). A few thicker diameter axons (thick arrow) were observed in CC (**e**). Scale in c=a,b,d; e=f-g.

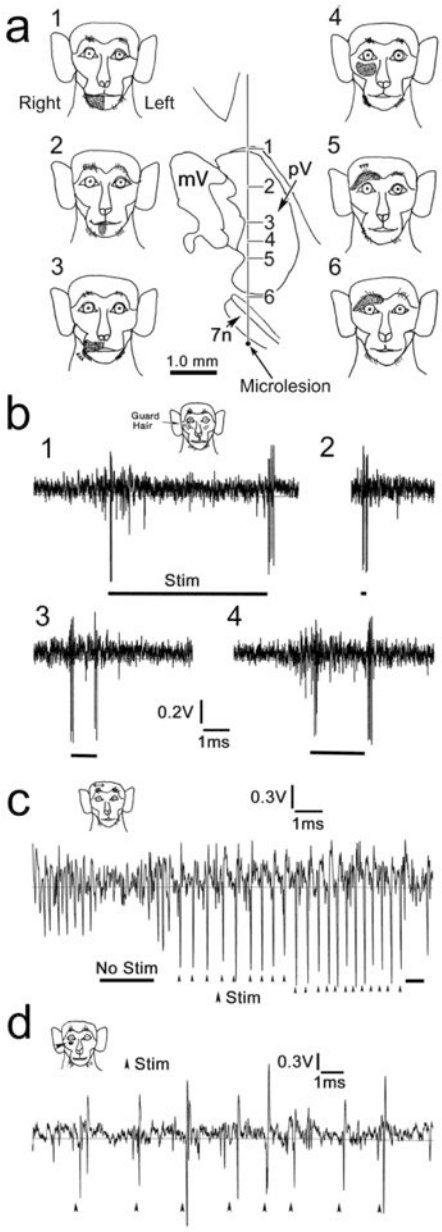

Figure 8.

Face receptive fields in pV. **a.** Upside down topography of face representation in pV is demonstrated by illustrations of 6 receptive fields encountered on a single electrode pass through the right nucleus. The bottom of the track was marked with a microlesion. **b-d.** Examples of neuronal activity found in pV. Receptive fields are indicated on monkey icons. The fast adapting unit shown in **b** responds to bending an infraorbital guard hair (Stim). Responses $\mathbf{b}_{1\text{-}4}$ demonstrate that there is little response while the hair is continuously bent, without regard to bending time. Instead, the unit responds for the initial bending, and when the hair is released. Unit **c** responds to stroking the eyebrow in either direction, and follows (arrowheads) the stimulation (Stim) faithfully. Unit **d** had a small infraorbital receptive field, and produced a single action potential each time a Von Frey hair touched the skin.

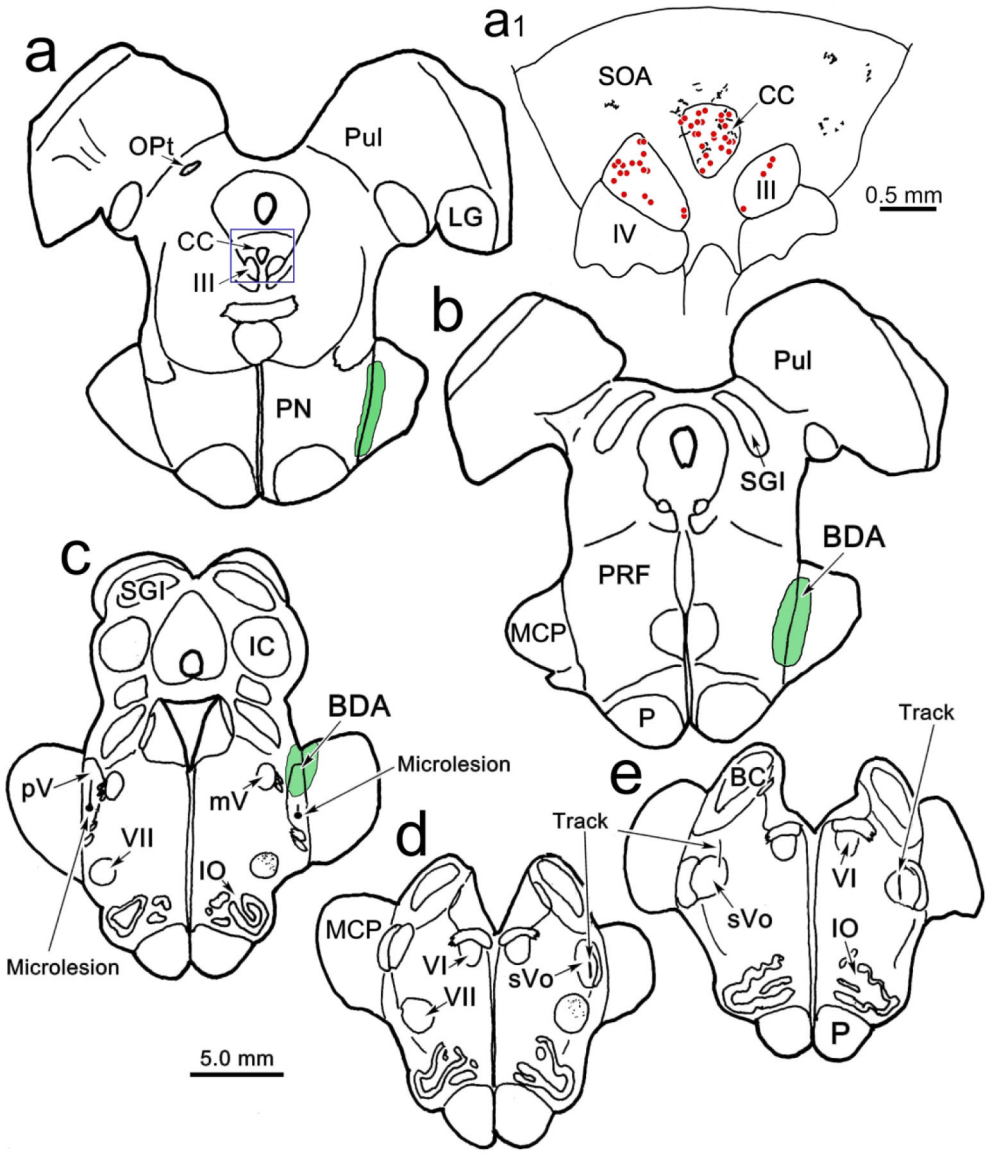

Figure 9.

Distribution of the peri-oculomotor terminal field following a physiologically localized (see Fig. 8) BDA injection (Case 6). Microlesions (**c**) and tracks (**d-e**) indicate areas in which neurons with receptive fields on the face were recorded in pV. This information was used to make a BDA injection in rostral pV (**c**), which spread further rostrally along the medial border of the middle cerebellar peduncle (MCP)(**a-b**). As shown in the higher magnification insert (**a**$_1$), this injection produced terminal labeling (stipple) in SOA and CC. This animal also received a WGA-HRP injection in the levator and superior rectus muscles that retrogradely labeled motoneurons (dots) in III and CC.

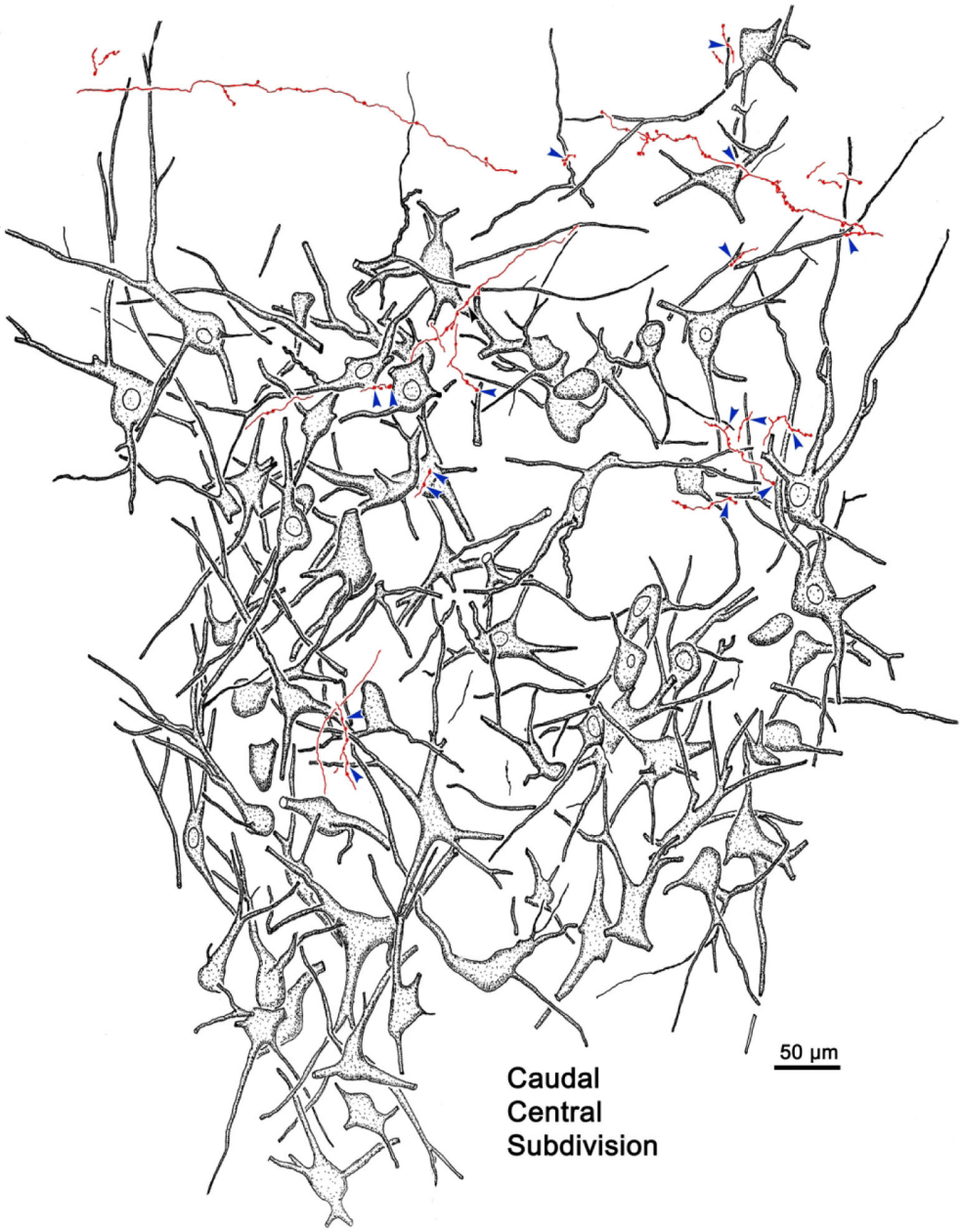

Figure 10.

Relationship of BDA labeled axon terminal arbors from the physiologically localized injection (Fig. 9; Case 6) with retrogradely labeled levator motoneurons (shaded) in CC. Terminals show close associations (arrowheads) with the motoneurons.

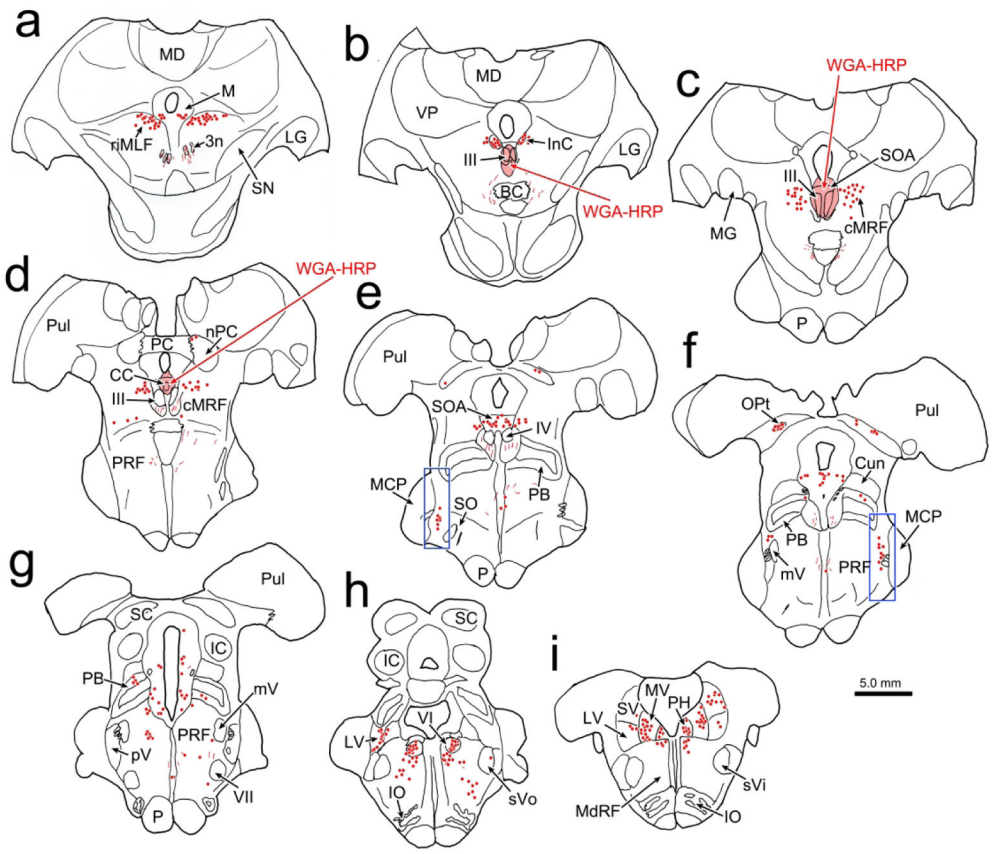

Figure 11.

Distribution of neurons supplying the oculomotor complex. The injection of WGA-HRP involved III, CC and SOA (**b-d**). It also spread into the overlying periaqueductal gray(**c-d**), and the region immediately ventral to III (**b**). The distribution of retrogradely labeled neurons (dots) is plotted from the diencephalon (**a**) through the medulla (**i**). Note the retrogradely labeled cells immediately rostral to pV (**e-f**). The boxed areas in **e-f** are shown in figure 12.

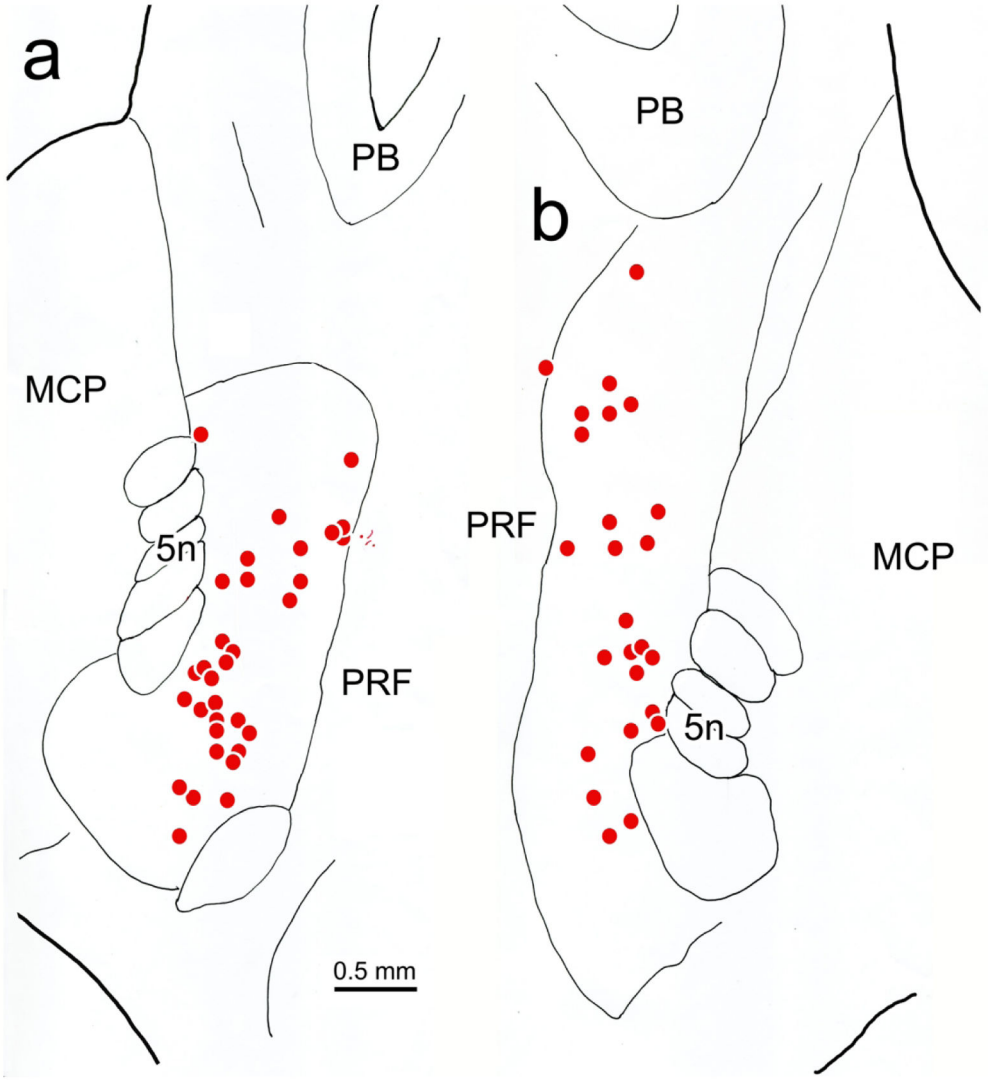

Figure 12.

Distribution of trigemino-oculomotor neurons. Retrogradely labeled neurons (dots) from the oculomotor complex injection shown in figure 11 are found immediately rostral to the left (**a**) and right (**b**) pV, just medial to bundles of trigeminal nerve (5n) fibers.

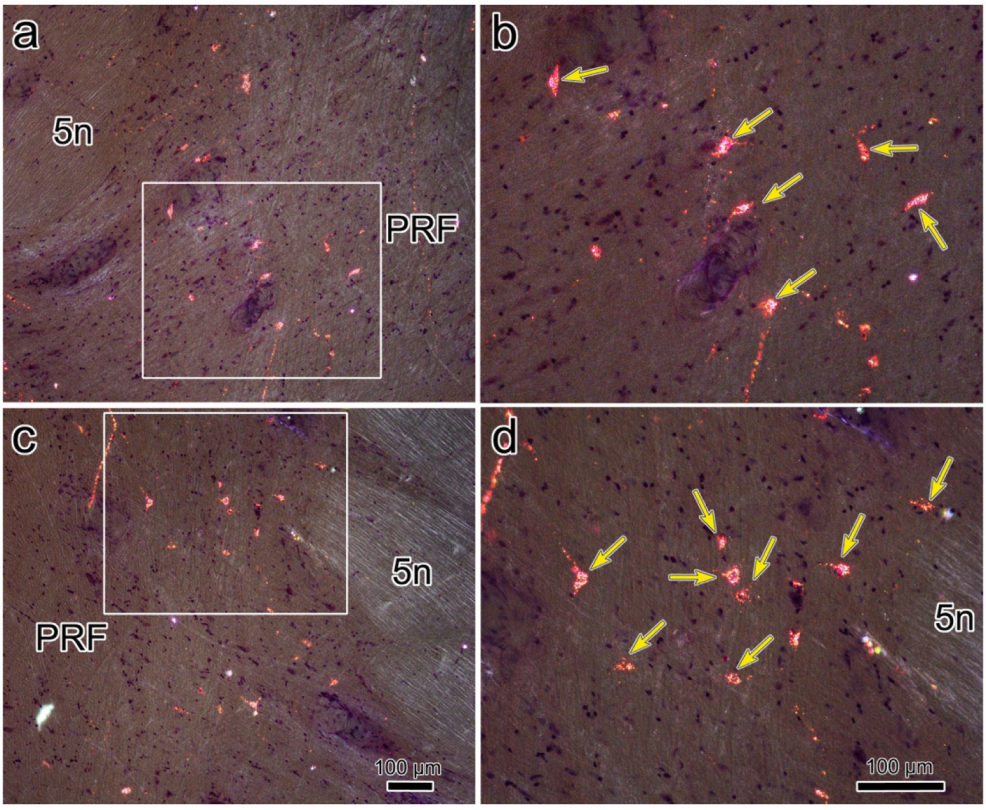

Figure 13.

Retrograde labeling of trigemino-oculomotor neurons demonstrated with crossed polarizer illumination (injection shown in Fig. 11). The region containing the labeled cells is indicated at low magnification for the left (**a**) and right (**c**) sides. The boxed areas in **a** and **c** are shown in the higher magnification views in **b** and **d**, respectively. Numerous retrogradely labeled cells (arrows) are present. Scale in c=a, d=b.

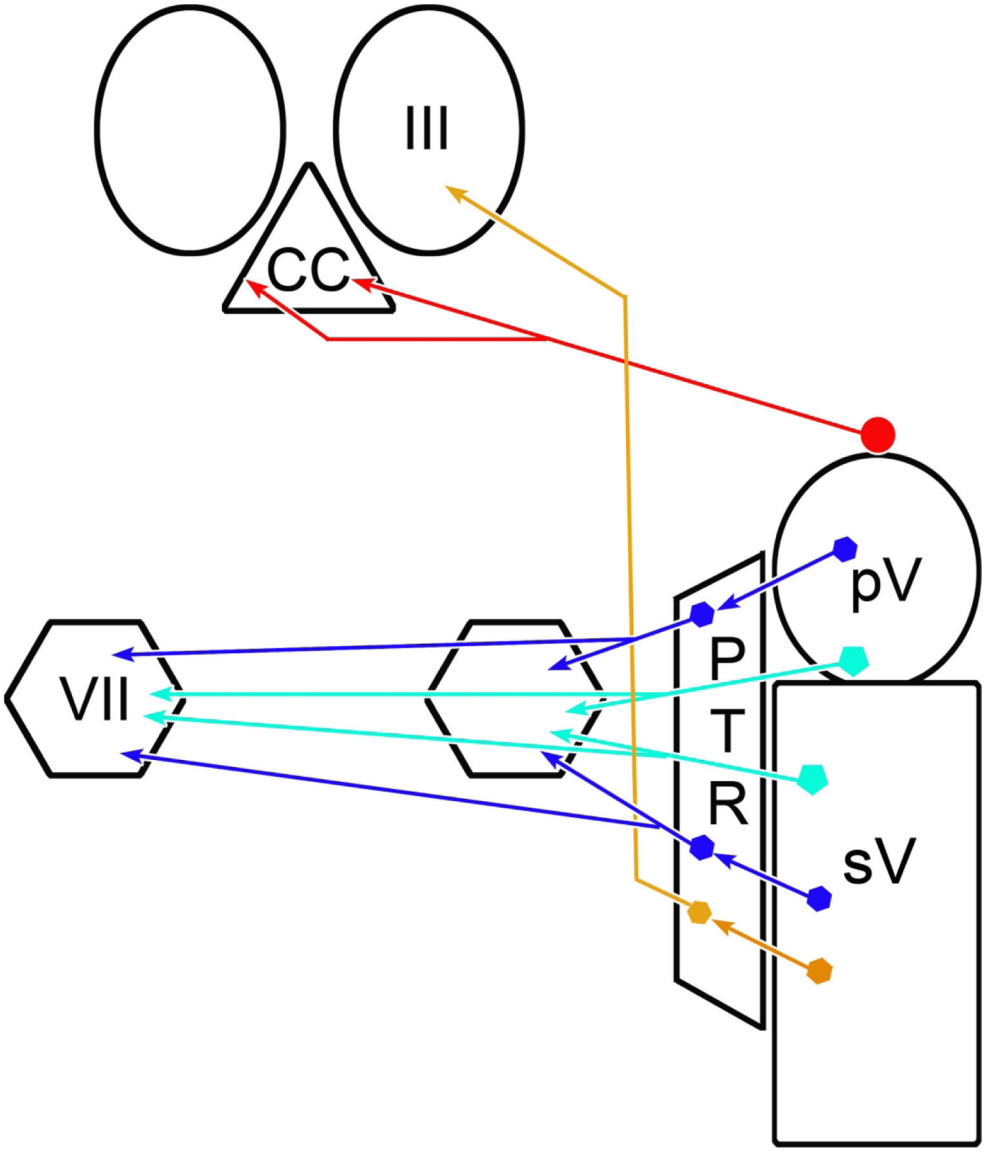

Figure 14.

Summary diagram showing trigeminal pathways underlying the blink reflex. The inhibitory trigemino-oculomotor pathway to the levator motoneurons located in the caudal central subdivision (CC) is shown in red. The monosynaptic excitatory pathways to the orbicularis oculi motoneurons in the facial nucleus (VII) are shown in light blue and the disynaptic excitatory pathways by way of the paratrigeminal reticular formation (PTR) are shown in dark blue [Data from May and Warren, 2021]. A putative excitatory pathway from the caudal portion of PTR to the oculomotor nucleus (III), which would cause retraction of the globe during a blink, is shown in brown.